Differentiation 140 (2024) 100813

Contents lists available at ScienceDirect

Differentiation

journal homepage: www.elsevier.com/locate/diff

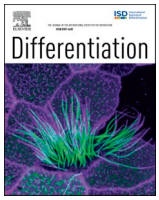

Fgf17: A regulator of the mid/hind brain boundary in mammals

Zane Oberholzer *, Chiron Loubser, Natalya V. Nikitina

School of Molecular and Cell Biology, University of the Witwatersrand, Private Bag 3, Wits, 2050, Johannesburg, South Africa

ARTICLE INFO

Keywords:
FGF
FGF17 gene
Mouse mutant
Mutations
Development
Rostral patterning centre
Midbrain-hindbrain boundary
Inferior colliculus
Dorsal frontal cortex
Cancer
Congenital hypogonadotropic hypogonadism
Kallmann syndrome
Pituitary stalk interruption syndrome

ABSTRACT

The Fibroblast growth factor (FGFs) family consists of at least 22 members that exert their function by binding and activating fibroblast growth factor receptors (FGFRs). The *Fgf8/FgfD* subfamily member, *Fgf17*, is located on human chromosome 8p21.3 and mouse chromosome 14 D2. In humans, FGF17 can be alternatively spliced to produce two isoforms (FGF17a and b) whereas three isoforms are present in mice (Fgf17a, b, and c), however, only Fgf17a and Fgf17b produce functional proteins. Fgf17 is a secreted protein with a cleavable N-terminal signal peptide and contains two binding domains, namely a conserved core region and a heparin binding site. *Fgf17* mRNA is expressed in a wide range of different tissues during development, including the rostral patterning centre, midbrain-hindbrain boundary, tailbud mesoderm, olfactory placode, mammary glands, and smooth muscle precursors of major arteries. Given its broad expression pattern during development, it is surprising that adult *Fgf17*$^{-/-}$ mice displayed a rather mild phenotype; such that mutants only exhibited morphological changes in the frontal cortex and mid/hind brain boundary and changes in certain social behaviours. In humans, *FGF17* mutations are implicated in several diseases, including Congenital Hypogonadotropic Hypogonadism and Kallmann Syndrome. *FGF17* mutations contribute to CHH/KS in 1.1% of affected individuals, often presenting in conjunction with mutations in other *FGF* pathway genes like *FGFR1* and *FLRT3*. *FGF17* mutations were also identified in patients diagnosed with Dandy-Walker malformation and Pituitary Stalk Interruption Syndrome, however, it remains unclear how *FGF17* is implicated in these diseases. Altered *FGF17* expression has been observed in several cancers, including prostate cancer, hematopoietic cancers (acute myeloid leukemia and acute lymphoblastic leukemia), glioblastomas, perineural invasion in cervical cancer, and renal cell carcinomas. Furthermore, FGF17 has demonstrated neuroprotective effects, particularly during ischemic stroke, and has been shown to improve cognitive function in ageing mice.

1. Introduction

The Fibroblast growth factor 17 (*FGF17*) belongs to the *Fgf8/FgfD* subfamily of FGF signalling molecules, which includes *FGF8*, *FGF17*, *FGF18* and *FGF24*. Members of the *FgfD* subfamily are paracrine signalling molecules (Jovelin et al., 2010), which exert their actions by binding to transmembrane tyrosine kinase receptors (FGFR1-4) (Ornitz and Itoh, 2015).

Fgf17 transcripts were first identified in rat, mouse and humans by Hoshikawa et al. (1998) and in zebrafish by Cao et al. (2004) A single *fgfD*-like gene is present in the genome of the chordates *Ciona intestinalis* (Satou et al., 2002) and amphioxus (Meulemans and Bronner-Fraser, 2007). This gene appears to have undergone a duplication to produce *fgf8* and *fgf17* in the lineage leading to ancestral vertebrates, and further duplicated in teleost fishes, however the second copy of *fgf17* was lost (Jovelin et al., 2010). There was a secondary loss of *fgf17* in the genome of *Xenopus tropicalis* (Lea et al., 2009; Goutam et al., 2023). Interestingly, *FGF17* was also lost independently from the genomes of some avian clades, most notably Galliformes (chicken) and Passeriformes (zebra finch) (Abramyan, 2015). Most of the information about the function and expression of *Fgf17* discussed in this primer is derived from studies in mammals and teleost fishes.

Fgf17 is expressed in multiple tissues during development, including the midbrain-hindbrain boundary, tailbud mesoderm, olfactory placode, mammary glands, and smooth muscle precursors of major arteries. In both mammals and zebrafish, it functions in the establishment of the midbrain-hindbrain boundary. In humans, mutations in *FGF17* are associated with Congenital hypogonadotropic hypogonadism/Kallmann Syndrome. Expression of *FGF17* is also altered in several cancer types.

This primer will delve deeper into the genomic structure and expression patterns of *Fgf17* as well as its functions during development. Lastly, this primer will look at how mutations in *FGF17* contribute to

* Corresponding author. School of Molecular and Cell Biology University of the Witwatersrand, Private Bag 3, Wits, 2050, Johannesburg, South Africa.
E-mail addresses: 909187@students.wits.ac.za (Z. Oberholzer), chiron.loubser@wits.ac.za (C. Loubser), natalya.nikitina@wits.ac.za (N.V. Nikitina).

https://doi.org/10.1016/j.diff.2024.100813
Received 30 June 2023; Received in revised form 6 September 2024; Accepted 12 September 2024
Available online 16 September 2024

human disease.

2. Gene structure

Fgf17 is part of the *Fgf8/FgfD* subfamily, which contains the paracrine (canonical) *Fgfs*. Its ancestral gene, *Fgf8-like*, in addition to all other ancestral paracrine Fgfs, was generated from *Fgf14-like* by gene duplication. All paracrine subfamilies in turn expanded via two large-scale genome duplication events to contain 3-4 members, i.e., *Fgf8/Fgf17/Fgf18* (Itoh and Ornitz, 2008).

FGF17 has been identified in both humans (8p21.3; GRCh38) and mice (14 D2 in mice; GRCm39). The human and mouse genes share 98.6% identity in the coding sequence. *FGF17* gene contains sequences for three versions of exon 1 (1A, 1B and 1D), which can be alternatively spliced to produce three isoforms in mice (Fgf17a, b, and c) and two in humans (FGF17a and b) (Xu et al., 1999). The last two exons (exon 2 and exon 3) are the same in all three alternatively spliced versions of FGF17. The mouse isoform c contains a stop codon at the end of exon 1B and is therefore assumed to not produce a functional protein (Xu et al., 1999) (Fig. 1).

Characteristic of all paracrine FGFs, FGF17 is a secreted protein with a cleavable N-terminal signal peptide and contains two binding domains. The first of these, a 123-amino acid conserved core region, adopts a cylindrical barrel structure consisting of 12 antiparallel β strands that bind the c isoforms of FGFR 1–3 and FGFR4 (Xu et al., 2000; Olsen et al., 2006; Zhang et al., 2006). The second domain is a heparin binding site that binds to extracellular heparin/heparin sulfate proteoglycans which functions as co-factors for efficient activation of FGFRs (Mohammadi et al., 2005; Raman et al., 2005; Li et al., 2016) (Fig. 1).

Fgf17 expression is spatially regulated by two evolutionary conserved shadow enhancers (Visel et al., 2007) which are active in the forebrain during development: an intragenic enhancer (Vista enhancer element # 782) active in the septum, and an intergenic enhancer (Vista enhancer element # 781) located between *Fgf17* and its neighbouring gene, *Ebp4.9*, active in the telencephalic roof plate and the septum. Although both enhancers contain Tcf/Lef transcription factor binding sites (transcriptional mediators of Wnt/β-catenin signalling), only the intergenic enhancer is repressed directly by Wnt/β-catenin signalling, as opposed to the intragenic enhancer which lacks the ability to bind Lef (Hasenpusch-Theil et al., 2017). During the development of the mesencephalon and rostral metencephalon (precursors to the midbrain and cerebellum) *Fgf17* expression is additionally maintained by *Fgf8* (Chi et al., 2003). In zebrafish, *fgf17* has been shown to be dependent on *pax2.1* and *fgf8* expression during midbrain-hindbrain boundary development (Reifers et al., 2000).

3. Expression studies

Expression of *Fgf17* has been investigated by using RT-PCR and RNA *in situ* hybridisation in several mammalian models (mouse, rat), as well as in zebrafish and stickleback. *Fgf17* mRNA is expressed in a wide range of different tissues, and frequently overlaps with *Fgf8* and/or *Fgf18* (Fig. 2).

3.1. *Fgf17 expression during mouse embryonic development*

Key areas of expression in the mouse embryo include tailbud mesoderm, midbrain-hindbrain boundary, olfactory placode, large arteries, tooth ectoderm and AER (apical ectodermal ridge) of the limb buds (see Fig. 2 for detailed timeline).

Fgf17 expression is first seen in the developing gastrula from E6.25–6.5 (Maruoka et al., 1998). At E7.5-E7.75, *Fgf17* expression becomes restricted to the posterior primitive streak and presomitic mesoderm (Maruoka et al., 1998; Boylan et al., 2020).

Brain development. In the midbrain -hindbrain junction, *Fgf17* expression is first detectable at the 6 somite stage (~E8.5) (Liu et al.,

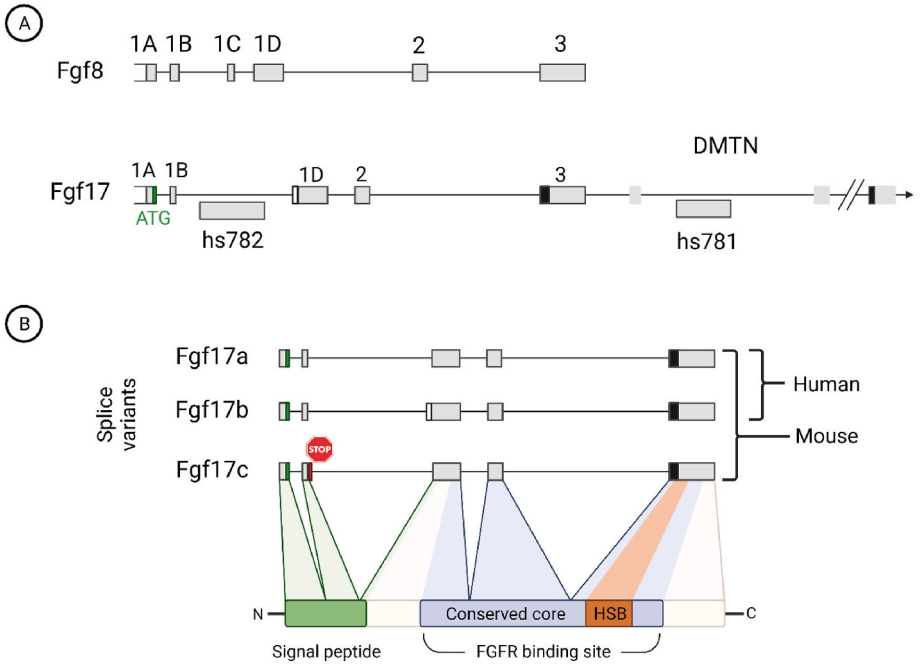

Fig. 1. *Fgf17* gene structure. A) *Fgf8* and *Fgf17*, two members of the *Fgf8* subfamily. *Fgf17* was derived from *Fgf8* via whole genome duplication. The sub-exons 1A-1D represent the alternatively spliced first exons for both *Fgf8* and *Fgf17* which produce multiple protein isoforms in humans and mice. A, bottom: *Fgf17* gene structure in humans on chromosome 8. Two experimentally validated enhancer elements for *Fgf17* expression. DMTN: Dematin actin binding protein. B) Human *FGF17* and mouse *Fgf17* splice forms. Mice have three isoforms, *Fgf17a-c*, while humans only have *FGF17a* and *b*. The mouse *Fgf17c* isoform has a stop codon in the extended 1B sub-exon. The *Fgf17b* isoforms for both human and mouse have an extended 1D sub-exon; 33 nucleotides/11 amino acids. B, bottom: FGF17 protein structure. Green block is the signal peptide. The blue block is the FGFR binding region with the heparin binding site (orange block). Grey blocks represent exons. Green block, the start codon in sub-exon 1A. Red box, the premature stop codon in FGF17c. Lines represent introns. Figure created with BioRender.com.

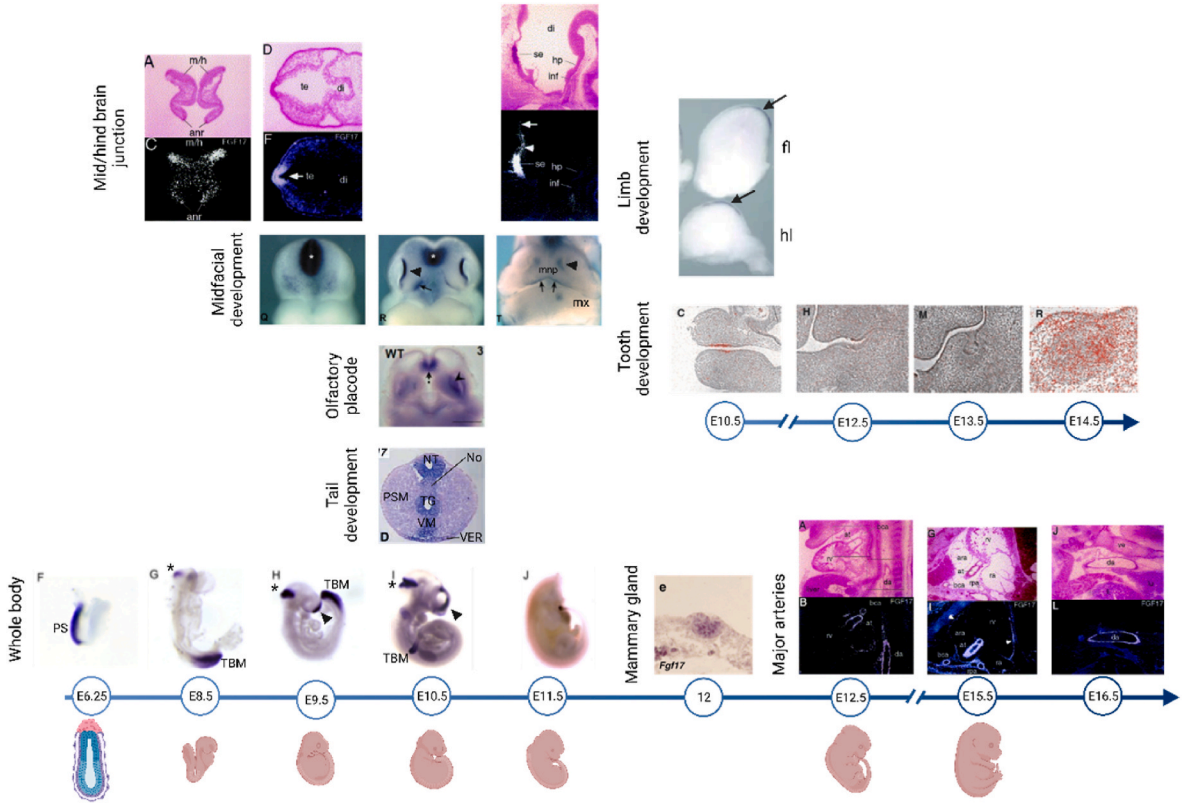

Fig. 2. ***Fgf17*** **expression during mouse development from stages E6.26 to E16.5 of development. Whole body:** *Fgf17* is expressed in the presomitic mesoderm (PS) at stage E6.26 (F). Expression in the tail bud mesoderm (TBM) is observed from E8.5-E11.5 (G, H, I, J), the mid/hind brain (*) from E8.5–10.5 (G, H, I) and in the prospective telencephalic commissural plate (arrowhead) from E9.5–10.5 (H,I). Image adapted from (Boylan et al., 2020) with permission. **Tail development:** Expression is localized to the posterior two thirds of the ventral ectodermal ridge (VER), the tail bud mesoderm (TBM) and in midline structures: the neural tube (NT), the ventral mesoderm (VM) the tail gut (TG). Abbreviations: No, notochord; PSM, presomitic mesoderm; ectodermal ridge. Image adapted from (Goldman et al., 2000) with permission. **Olfactory placode:** At E10.5, expression is observed in the medial olfactory placode (arrowhead) in addition to the telencephalic commissural plate (dotted arrow). Image adapted from (Miraoui et al., 2013) with permission. **Midfacial development:** At E9.5 (I) expression is observed in the ectoderm covering the midfacial region and in the underlying forebrain (I, asterisks). At E10.5 and E11.5 *Fgf17* expression is restricted to the medial olfactory placode (R and T, arrowheads), and the along the oral edge of the medial nasal process (mnp; R and T, arrow). Image adapted from (Bachler and Neubüser, 2001) with permission. **Mid/hind brain junction:** At E8.5 is expressed in the midbrain-hindbrain junction (A and C, m/h) Anr, anterior neural ridge. At E9.5 (D and F), *Fgf17* expression is only observed in a small domain at the transition between the dorsal telencephalon (te) and diencephalon (di). At E11.5 (G and I) expression is observed in the septal neural epithelium (se) and telencephalon-diencephalon junction (arrowhead). Expression is additionally observed in the dorsal diencephalon (I, arrow). Abbreviations: hp, hypothalamus and inf, infundibular recess. Figure adapted from (Xu et al., 1999) with permission. **Mammary gland:** *Fgf17* expression is restricted to the mammary epithelium. Figure adapted from (Eblaghie et al., 2004) with permission. **Major arteries:** At all developmental stages, E12.5 (A and B), E15.5 (G and I) and E16.5 (J and L), expression is observed in all major arteries and pericardium (I, arrows). Abbreviations: A and B, aortic arch (at), brachiocephalic artery (bca), descending aorta (da) and right ventricle (rv); G and L, auricular part of left atrium (ara), right pulmonary artery (rpa), right atrium (ra); J and L, vertebral column (ve), liver (li) and lung (lu). Figure adapted from (Xu et al., 1999) with permission. **Secondary timeline: Tooth development:** *Fgf17* expression is restricted to the presumptive tooth epithelium at E10.5 (C). Weak expression was observed in the cervical loop (R). Figure adapted from (Porntaveetus et al., 2011) with permission. **Limb development:** *Fgf17* is expressed in the posterior two-thirds of the apical ectodermal ridge in both the fore limb (fl) and hind limb (hl) as indicated by the arrow. Image adapted from (Sun et al., 2000) with permission. Figure created with BioRender.com.

2003). By E9.5, the expression domain of *Fgf17* extends into the posterior midbrain and anterior hindbrain which persists until E12.5 (Xu et al., 1999; Xu et al., 2000; Liu et al., 2003). From E12.5- E14.5, *Fgf17* expression becomes restricted to the mid/hindbrain junction (Hoshikawa et al., 1998; Xu et al., 1999; Xu et al., 2000). At E16.5, *Fgf17* expression was detected in the velum medullare (VM) (tissue derived from the mid/hindbrain junction that connects the inferior colliculus (IC) with the cerebellum) (Yaguchi et al., 2009). *Fgf17* expression is not detected after E16.5 in the mid/hindbrain junction (Yaguchi et al., 2009).

Fgf17 expression is first detected at E8.5 in the anterior neural ridge (Xu et al., 1999; Xu et al., 2000). From E9.5-E12.5, *Fgf17* is expressed in the midbrain, along the rostral patterning centre/telencephalic commissural plate as well as a small domain at the transition between the dorsal telencephalon and diencephalon (Maruoka et al., 1998; Xu et al., 1999; Xu et al., 2000; Cholfin and Rubenstein, 2007). Fate mapping of *Fgf17*$^{+}$ cells show that at E18.5, *Fgf17*$^{+}$ cells also contribute to the septum, diagonal band of Broca, olfactory bulb, mitral cell layer and the dorsomedial cortex (Hoch et al., 2015).

Mid facial development. *Fgf17* expression is first detected in the ectoderm covering the presumptive midfacial region at E9.5 (Bachler and Neubüser, 2001). From E10.5-E11.5, *Fgf17* expression is restricted to the ectoderm of the nasal pits and the medial nasal process. *Fgf17* expression is also detected in the maxilla at E15.5 (Xu et al., 1999).

Fgf17 expression in other structures. *Fgf17* expression is observed in the presumptive molar at E10.5 (Porntaveetus et al., 2011). *Fgf17* is expressed in the dental epithelium from E11.5–13.5 (Kettunen et al., 2011; Porntaveetus et al., 2011). While *Fgf17* expression cannot be detected at E13.5 in the developing molar, *Fgf17* expression is detected again at E14.5 in the cervical loop epithelium and the surrounding mesenchyme (Kettunen et al., 2011; Porntaveetus et al., 2011). *Fgf17* expression was not detected in the molar at E18.5 or in new-born mice

(Porntaveetus et al., 2011). Interestingly, while *Fgf17* expression is not detected in the presumptive incisor region at E10.5, it is expressed in epithelium of the labial cervical loop of the developing incisor at E16.5 (Porntaveetus et al., 2011).

Fgf17 is seen in the developing tail bud at E9.5 (Boylan et al., 2020). At E10.5, whole mount *in situ* hybridisation showed *Fgf17* expression in the ventral ectodermal ridge of the tail bud and in the tail bud mesenchyme, while transverse sections of the tailbud showed *Fgf17* expression in the neural tube, tail gut, ventral mesoderm and the ventral ectodermal ridge (Maruoka et al., 1998; Goldman et al., 2000).

Fgf17 is expressed weakly in the posterior AER of the developing limb bud of E10.5-E12 mice (forelimb and hindlimb) (Lewandoski et al., 2000; Sun et al., 2000; Mariani et al., 2008). *Fgf17* is expressed in the mammary epithelium of the developing mammary gland at E12 (Eblaghie et al., 2004). *Fgf17* expression is also present in the walls of the major arteries (aortic trunk, brachiocephalic artery, pulmonary artery and descending aorta) from E12.5-E16.5 (Xu et al., 1999). Interestingly, *Fgf17* expression is not detected in any veins (Xu et al., 1999).

3.2. Fgf17 expression in mouse adult tissue

Fgf17 RNA transcripts were found in all major tissue systems of 8–9 week old male mice (central nervous system, endocrine system, GI system, metabolic system, immune system, reproductive system, cardiovascular system and skeletal system) (Tacer et al., 2010). *Fgf17* expression was not detected in the adrenal gland, tongue, duodenum, jejunum, ileum, white adipose tissue, uterus, vas deferens, heart and bone (Tacer et al., 2010).

3.3. Expression in zebrafish

In zebrafish, the gene initially annotated as *fgf17* (*fgf17a*) (Reifers et al., 2000) was since identified as a second paralogue of the teleost *fgf8* (Jovelin et al., 2007), which arose in the course of teleost-specific WGD. *Fgf17b* is now considered the sole zebrafish orthologue of the tetrapod *fgf17* (Cao et al., 2004).

In zebrafish, *fgf17* expression was examined by *in situ* hybridisation during the first 24hrs of embryonic development. The *fgf17* expression occurs in two phases. During the early phase, *fgf17* transcripts are found in the dorsal margin, and then became restricted to the embryonic shield. There was a dip in *fgf17* expression by 75% epiboly. During the second phase of expression, the transcripts were detected in the presomitic mesoderm and somites, as well as in the dorsal telencephalon (Cao et al., 2004).

Fluorescent *in situ* hybridization performed on embryos at 30 hpf showed *fgf17* expression in the endoderm of the pharyngeal pouch as well as in the mesoderm adjacent to the pharyngeal pouch (Jin and Choe, 2024).

4. Functional studies, mutants and phenotypes

Generation of the *Fgf17* knockout mouse was first reported by Xu et al. (Xu et al., 2000). Mice homozygous for the inactive $Fgf17^{neo}$ allele were viable and displayed no obvious morphological abnormalities (see Table 1 for the phenotypes of $Fgf17^{-/-}$ mouse mutants). The brains of the homozygous mutant mice exhibited reduction in the size of some brain areas, including the most caudal part of the midbrain, the inferior colliculus and the vermis cerebellum (Xu et al., 2000) (Fig. 3). Even though the frontal cortex (FC) of $Fgf17^{-/-}$ mice appeared to have normal morphology, detailed examination of the subdivision of the FC using a panel of molecular markers revealed expansion of the parietal cortex markers into dorsal FC regions (Cholfin and Rubenstein, 2007) (Fig. 3). Phenotypically, this manifested in abnormalities in certain types of social behaviour (Scearce-Levie et al., 2008).

Given that *Fgf17* is expressed in a wide range of different tissues throughout embryonic development (Fig. 2), the relatively minor phenotype of the $Fgf17^{-/-}$ mice may be surprising. However, both *Fgf8* and *Fgf18* are frequently co-expressed with *Fgf17*, and show high degree of functional redundancy, such that $Fgf17^{-/-}$ in combination with the loss of one *Fgf8* allele results in increasingly severe phenotypes (Xu et al., 2000; Cholfin and Rubenstein, 2008).

4.1. Fgf17 is important for growth and differentiation of the cerebellum

Fgf17 has different functions throughout embryonic development of the mid/hindbrain. Since *Fgf17* is expressed prior to E10 in the isthmus, it is believed that *Fgf17* functions as an organizer in the isthmus (midbrain/hindbrain boundary); participating in the MHB gene cascade that patterns adjacent structures (Xu et al., 1999; Xu et al., 2000; Liu et al., 2003). The rostral side of the midbrain/hindbrain boundary develops into the inferior colliculus (IC) whereas the caudal side of the midbrain/hindbrain boundary develops into the vermis cerebellum (Bally-Cuif and Wassef, 1995; Liu et al., 2003). It should be noted that *Fgf17* role as an organizer has not been functionally demonstrated though, largely due to the overlapping functions of *Fgf8*, *Fgf17* and *Fgf18* in the isthmus (Lee et al., 1997; Liu and Joyner, 2001; Liu et al., 2003).

After E10, *Fgf17*, acts as a growth factor by promoting the proliferation of the vermis neuroepithelium (Xu et al., 2000). $Fgf17^{-/-}$ mice which lack the translation initiation site and two exons encoding the signal peptide of *Fgf17*, showed no changes in the expression pattern of several genes (*Wnt1*, *En2*, *Pax5* and *Otx2*) essential in midbrain/hindbrain patterning at E12.5, however, detection of BrdU in labelled sections taken from the medial part of the cerebellar plate (region where vermis anlage precursor cells are found) of E10.5-E12.5 mice showed a progressive decrease in cell proliferation and a thinner neuroepithelium in $Fgf17^{-/-}$ mice compared to control mice over the two day time period (Xu et al., 2000). In contrast, TUNEL assays performed on sections taken from the of the cerebellar plate of E12.5 wild-type and $Fgf17^{-/-}$ mice showed no significant changes in cell death (Xu et al., 2000). Furthermore, Liu et al., showed that ectopically expressing *FGF17* in the midbrain of chick embryos (HH9-12) via electroporation resulted in the expansion of the midbrain (Liu et al., 2003). *In-situ* hybridisation of *GBX2* and *OTX2* on sections taken from the midbrain/r1 region 24 h after electroporation, showed no changes in expression, further supporting *Fgf17* role as a growth promoting factor that acts after the midbrain/hindbrain boundary has been established (Liu et al., 2003).

$Fgf17^{-/-}$ mice at postnatal day 2 (P2) and 2–3 months after birth displayed no morphological defects in the cerebellar hemisphere, however, the IC and the vermis cerebellum were smaller (Xu et al., 2000). Deformation-Based Morphometry analysis of P21 $Fgf17^{-/-}$ and control mice confirmed the size reduction of IC and anterior cerebellum but also detected a decrease in size of the olfactory bulb (Yu et al., 2011).

The IC functions as an important processing centre for auditory information and is involved in discriminating pitch, rhythm and sounds from different sources (Gruters and Groh, 2012). MEMRI (Manganese-enhanced MRI) imaging was performed on the IC of P21 $Fgf17^{+/-}$ and $Fgf17^{-/-}$ mice (Yu et al., 2005, 2011; Malheiros et al., 2015), where the control group for each phenotype (kept in a quite environment) was compared to mice stimulated with broadband sound spanning the auditory rage of mice (1–59 kHz) (Yu et al., 2011). While the signal intensities in the cochlear nuclei showed no differences between the genotypes, the signal intensities in the active IC were reduced in $Fgf17^{-/-}$ mice compared to $Fgf17^{+/-}$ mice (Yu et al., 2011). The decreased IC core activity is therefore not a result of changes in auditory input, but rather a reduction in the volume of the IC activated by auditory input. Further tonotopic analysis of 16-and 40-kHz activity patterns, which activate dorsal (lower frequencies) and ventral neurons (higher frequencies) respectively, showed significant alternations in $Fgf17^{-/-}$ mice with largely overlapping topologies compared to $Fgf17^{+/-}$ mice, which showed activation of well-separated domains along the dorsal-ventral axis of the IC. The altered tonotopic map in $Fgf17^{-/-}$ mice suggests that *Fgf17* may be involved in how the afferent

neurons are patterned, either directly or indirectly by regulating other molecules in the IC (Yu et al., 2011). Future studies involving axon-tracing in *Fgf17*$^{-/-}$ mutants could address this.

Since *Fgf17* has been shown to act as a growth factor after E12.5 and *Fgf17* expression extends into the region where the vermis cerebellum precursor cells are found, it was proposed that the tissue loss observed in the vermis was not due to patterning defects but decreased proliferation which resulted in the premature exhaustion of the precursor cells that give rise to this structure (Xu et al., 2000). Consistent with this, the vermis developed in a caudal to rostral direction and displayed greater tissue loss in the anterior region (Xu et al., 2000). Interestingly, Purkinje cells, which are essential to normal cerebellar functioning, exhibited premature differentiation at E14 in *Fgf17*$^{-/-}$ mice, suggesting *Fgf17* keeps Purkinje cells in a proliferative state (Xu et al., 2000; Masoli, Solinas and D'Angelo, 2015).

The vermis cerebellum and Purkinje cells are involved in maintaining whole-body posture and motor coordination, however, gait, motor-co-ordination and balance tests which were performed on 3–4 month old wild-type and *Fgf17*$^{-/-}$ mice showed no differences in their movements Xu et al., 2000; Scearce-Levie et al., 2008; Masoli, Solinas and D'Angelo, 2015; Park et al., 2018). This suggests that the alterations to the vermis cerebellum was of little functional consequence or that other regions of the central nervous system can compensate for these changes.

4.2. *Fgf17 is a key regulator of the dorsal frontal cortex patterning and social behaviours*

The rostral patterning centre/telencephalic commissural plate is situated at the midline of the anterior forebrain and is responsible for patterning the cerebral cortex into different domains. *Fgf17*$^{-/-}$ mice at P0 displayed no differences in the overall size of the cortex, however, the cortex of adult *Fgf17*$^{-/-}$ mice showed a slight reduction in size (Cholfin and Rubenstein, 2007, 2008). Histological analysis of the rostral telencephalon of *Fgf17*$^{-/-}$ mice at P0, P7 and P8 showed a decrease in the frontal cortex size. To discern whether any patterning defects were present, *in situ* hybridisation was performed on coronal sections of P0 *Fgf17*$^{-/-}$ mice using several genes that demarcate specific cortex subdivisions (Cholfin and Rubenstein, 2007, 2008). It was found that the dorsal frontal cortex was shifted medially with smaller dorsal, dorsolateral and dorsomedial subdivisions whereas the parietal and occipital cortex domains expanded into the frontal cortex domain (Cholfin and Rubenstein, 2007, 2008). Interestingly, the ventral frontal cortex was unaffected, suggesting *Fgf17* has a selective role in patterning the dorsal frontal cortex (Cholfin and Rubenstein, 2007, 2008). Additionally, while there was a reduction in the number of EphA2-positive and Drd4-positive neurons, their pathfinding abilities were not altered. The reduced number of projections, however, could influence the neural circuits involved in reward, cognition, and social behaviour (Cholfin and Rubenstein, 2007, 2008). Analysis of P40 and 6 month old *Fgf17*$^{-/-}$ mice showed that these early embryonic alterations persist into adulthood (Cholfin and Rubenstein, 2007, 2008).

Social recognition tests were performed on *Fgf17*$^{+/+}$, *Fgf17*$^{+/-}$ and *Fgf17*$^{-/-}$ mice that were 4–8 months old (Scearce-Levie et al., 2008). The interaction times between male *Fgf17* mutants and wildtype (*Fgf17*$^{+/+}$) ovariectomized females were measured. All *Fgf17* genotypes responded similarly: initially showing interest in the female and then progressively interacting less with the female (Scearce-Levie et al., 2008). After a new wildtype ovariectomized female was introduced, *Fgf17*$^{+/+}$, *Fgf17*$^{+/-}$ mice interacted similarly as with the first female, however, *Fgf17*$^{-/-}$ mice lacked a resurgence of interest in the new female and spent significantly less time interacting with the new female (Scearce-Levie et al., 2008). In a second social recognition test, same-genotype, opposite-sex pairs of mice were placed in an environment, filled with novel stimuli for 2 h (Scearce-Levie et al., 2008). During the first hour of the experiment, all genotypes had similar interaction times, however, during the second hour of the experiment, *Fgf17*$^{+/+}$, *Fgf17*$^{+/-}$ mice pairs spent more time interacting with each other while *Fgf17*$^{-/-}$ mice spent less time interacting with each (Scearce-Levie et al., 2008).

This altered social behaviour cannot be attributed to any locomotion, olfactory or cognitive impairments, reduced explorative activity, changes in emotionality or an altered fear perception (Scearce-Levie et al., 2008). The reduced interaction time with the second novel female suggests *Fgf17*$^{-/-}$ mice have an impaired ability to compare and respond to new social information, which is regulated by the medial prefrontal cortex (Mitchell et al., 2006; Scearce-Levie et al., 2008). Fos staining (a marker of neuronal activation) was performed on brain sections of *Fgf17*$^{+/-}$ and *Fgf17*$^{-/-}$ mice after an experiment in which the mice were allowed to explore a novel environment with a novel partner for 2 h (Morgan and Curran, 1989; Scearce-Levie et al., 2008). Interestingly, *Fgf17*$^{-/-}$ mice displayed decreased Fos induction in the dorsomedial prefrontal cortex whereas other brain regions involved in social behaviour/response such as the frontal cortex, olfactory bulb and hippocampus showed normal Fos induction (Scearce-Levie et al., 2008). *Fgf17*$^{-/-}$ mice also displayed tissue loss in the vermis cerebellum and inferior colliculus, however, Fos induction in the vermis cerebellum did not show any differences between genotypes (Xu et al., 2000; Scearce-Levie et al., 2008). Fos induction in the inferior colliculus was not reported on. Since social behaviour/response is a complex behaviour

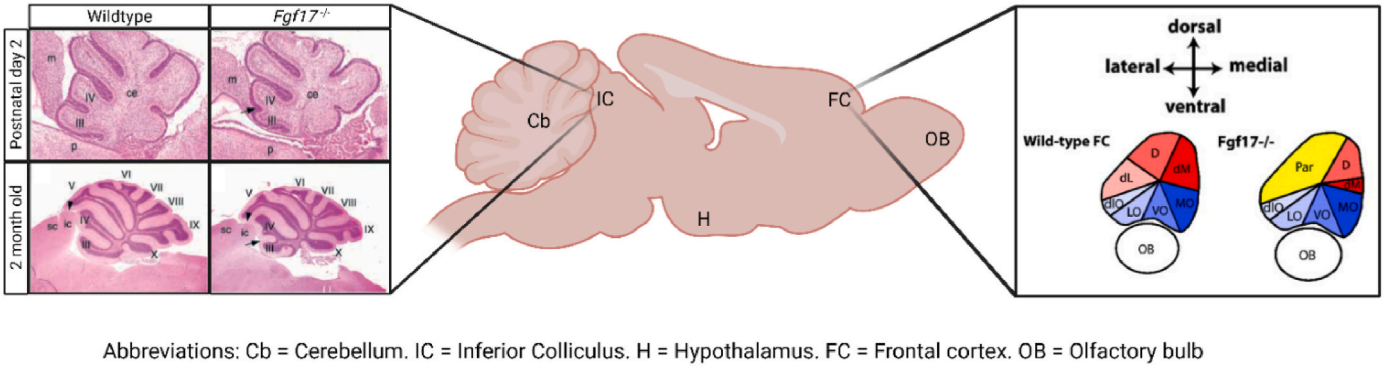

Abbreviations: Cb = Cerebellum. IC = Inferior Colliculus. H = Hypothalamus. FC = Frontal cortex. OB = Olfactory bulb

Fig. 3. Summary of *Fgf17*$^{-/-}$ mice phenotypes. Middle: Schematic of sagittal section taken of the brain showing major structures. **Left:** H&E staining of midsagittal section taken of *Fgf17*$^{-/-}$ and wildtype mice brains at P2 and 2 mo. The arrows indicate the smaller lobe III and the partial fusion of lobe III and IV (P2). At 2 mo, the arrowhead shows the smaller IC and the arrow shows the smaller lobe III. Figure adapted from (Xu et al., 2000) with permission. **Right:** Schematic depicting patterning defects of frontal cortex subdivisions between wildtype and *Fgf17*$^{-/-}$ mice. *Fgf17*$^{-/-}$ mice show patterning defects only in the dorsal frontal cortex and not the ventral frontal cortex subdivisions. In *Fgf17*$^{-/-}$ mice, the parietal cortex (Par) expands into the frontal cortex and the dorsal (D), dorsolateral (dL), and dorsomedial (dM) subdivisions of the frontal cortex are smaller. Figure adapted from (Cholfin and Rubenstein, 2007, 2008) with permission (Copyright (2007) National Academy of Sciences, U.S.A.). Figure created with BioRender.com.

involving several aspects of the brain, a more comprehensive analysis of the brain-auditory system in *Fgf17*$^{-/-}$ mice is required to elucidate the molecular mechanism behind the abnormal social behaviour these mice display.

4.3. Fgf17 supports oligodendrogenesis and memory in aging mice

In rat primary oligodendrocyte progenitor cell (OPC) cultures, addition of Fgf17 resulted in OPC proliferation and differentiation (Iram et al., 2022). When Fgf17 was infused into aged (twenty-month-old) mice over a seven day period, it resulted in increased OPC proliferation in the hippocampus and improved long-term memory performance (Iram et al., 2022). However, when anti-Fgf17 blocking antibodies were administered intracerebroventricularly to young mice (10-week-old mice), there was decreased Fos induction in the hippocampus and these mice showed impaired performance in two hippocampal-dependent cognitive tests (Y maze and contextual fear conditioning) (Iram et al., 2022). Taken together, this suggests that Fgf17 plays a role in oligodendrocyte proliferation and differentiation in the hippocampus, contributing to long-term memory performance.

4.4. FGF17 protects the blood-brain-barrier (BBB) during ischemic stroke in mice

The blood-brain barrier (BBB) is a highly selective semi-permeable barrier which provides a controlled microenvironment between the brain and the bloodstream (Kadry et al., 2020). Functioning as part of the neurovascular unit (McConnell and Mishra, 2022; Alkayed and Cipolla, 2023), the BBB is primarily formed by specialized endothelial cells held together by thigh- and adherens-junctions which, along with the basement membrane, pericytes and astrocyte end feet regulate the permeability and maintain the integrity of the BBB (Kadry et al., 2020; McConnell and Mishra, 2022). The BBB is the first part of the NVU damaged during stroke.

Stroke is a neurological disorder during which blood flow to the brain is disrupted due to obstruction (ischemic stroke, IS (Campbell et al., 2019)) or vessel rupture (haemorrhagic stroke). During IS, irreversible cell death occurs in the area directly affected, the ischemic core. Surrounding the core, is the ischemic penumbra; functionally impaired and reversibly injured tissue which may regain function if reperfused and is consequently the target for treatment (Salaudeen et al., 2024).

The breakdown of the BBB occurs soon after onset of stroke, during reperfusion and continues for days to weeks (Soldozy et al., 2023; Xue et al., 2023). At the onset of IS, oxygen and glucose deprivation due to reduced blood flow leads to ATP depletion, disruption of ion homeostasis producing cell swelling, cytotoxic edema, excitotoxicity, mitochondrial dysfunction and oxidative stress (reactive oxygen species formation). ROS, necrotic cells and damaged tissue initiates an inflammatory response which act to further disrupt the BBB. Matrix metalloproteinases (MMPs) in particular act to disrupt BBB integrity by degrading the extracellular components of the basement membrane as well as by tight junction protein dysregulation, translocation and degradation (Qin et al., 2022; Xue et al., 2023).

The main goal for IS treatment is to restore blood flow (reperfusion therapy) to the affected areas, within the first few hours after onset of IS. This involves either thrombolytic therapy (tissue plasminogen activator/tPA administration) to dissolve blood clots; or, mechanical thrombectomy to remove the clot (Xiong et al., 2022). Currently tPA is the only FDA approved treatment for acute IS, but can only be administered within 4.5 h of symptom onset due to increased risk of symptomatic intracranial haemorrhage (sIHC) (Charbonnier et al., 2021). A promising alternative; not yet FDA-approved, recombinant form of tPA (Tenectaplase) has shown promise as an alternative for acute IS treatment having not shown an increased risk of sIHC (Wang et al., 2024). Secondary to restoring blood flow is neuroprotection; modulation of any ischemia-induced processes which could irreversibly damage and/or kill

Table 1
Phenotypes of *Fgf17*$^{-/-}$ mouse mutants.

Genotype	Region of *Fgf17* gene targeted	Phenotype	Reference
Fgf17$^{-/-}$	Deletion of translation initiation start site and exon 1a and 1b of *Fgf17* (Xu et al., 2000).	• IC and vermis reduced in size (P2 & 2 mo) •No alterations observed in cerebellar hemispheres (P2 & 2 mo) •No patterning defects observed •Decreased proliferation observed in vermis neuroepithelium between E10.5-E12.5 •Premature differentiation of Purkinje cells (E13-14) •No gait defects (3–4 mo)	(Xu et al., 2000)
Fgf17$^{-/-}$		•Cortex slightly smaller in adult mice (P0) •Altered frontal cortex patterning (P0): o dorsal frontal cortex shifted medially with smaller dorsal, dorsolateral and dorsomedial subdivisions oparietal and occipital cortex domains expanded into the frontal cortex domain oventral frontal cortex unaffected •Patterning defects also present in adult (P40 and 6 mo) •Reduced number of EphA2-positive and Drd4-positive neurons in frontal cortex (P40 and 6 mo). •Pathfinding ability of neurons not altered (P40 and 6 mo)	(Cholfin and Rubenstein, 2007, 2008)
Fgf17$^{-/-}$		•Reduced size of IC, anterior cerebellum and olfactory bulb •Expansion of the anterior-medial rhinal fissure and hypothalamus •Decreased activity in active IC •Altered tonotopic map of IC	Yu et al. (2011)
Fgf17$^{-/-}$		•Reduced closed arm distance, elevated plus maze (4–8 mo) •Reduced ultrasonic vocalizations of mutant pups (P8) after isolation from mother •Abnormal social behaviour (4–8 mo): oDecreased social interaction between *Fgf17*$^{-/-}$ males and novel wildtype female, after extended period of time oDecreased neuronal activation (Fos staining) in dorsomedial prefrontal cortex after exploration of a novel environment with a novel partner	Scearce-Levie et al. (2008)

Abbreviations: IC = Inferior colliculus. P = Postnatal day. mo = month. E = Embryonic day.

neural tissue. Despite challenges in identifying neuroprotectants which translate into clinical practice (Haupt et al., 2022), there are numerous candidates in clinical trials (Haupt et al., 2023).

Multiple members of the FGF family have shown promise as potential candidates as neuroprotectants (Dordoe et al., 2021). Recently, Wang et al. (2024) highlighted FGF17s potential as a therapeutic strategy for addressing BBB disruption caused by reperfusion. Their study observed reduced expression of *Fgf17* in mice after middle cerebral artery occlusion (MCAO), patient serum and brain endothelial cells exposed to ischemic conditions (Huang et al., 2024). Administered intranasally, recombinant FGF17 treatment reduced the infarct area, improved sensorimotor deficits 24 h after MCAO and reduced tissue pathology with an observed reduction of neuronal necrosis and intracellular edema. Consistent with this observation, FGF17 treatment improved cerebral cortex perfusion and decreased BBB permeability due to the attenuated loss of tight and adherens junction proteins. FGF17 further reduced ROS production through the Nrf2/HO-1 pathway (Loboda et al., 2016); increasing Nrf2 accumulation in the nucleus and restored HO-1 expression levels. FGF17 treatment further protected against endothelial cell apoptosis, reducing the expression of apoptosis related proteins; caspase-3 and BAX (Saddam et al., 2024), while simultaneously attenuating apoptosis through the FGFR3/PI3K/AKT signalling pathway; increasing the phosphorylation of both FGFR3 and AKT after treatment, which mechanistically phosphorates and inactivates multiple downstream targets involved in apoptosis (Qin et al., 2022). FGF2 similarly attenuates neuronal apoptosis via the same FGF3/PI3K/AKT pathway after subarachnoid hemorrage (Okada et al., 2019).

4.5. *Fgf17 plays a role in limb development*

Even though *Fgf17* is expressed in the AER (Lewandoski et al., 2000), *Fgf17*$^{-/-}$ mice do not exhibit any limb defects (Xu et al., 2000). Other FGFs, including *Fgf8*, *Fgf9* and *Fgf4*, are co-expressed within the AER. Triple knockout *Fgf4, 9* and *17* mice did not exhibit any limb abnormalities, suggesting that only *Fgf8* has instructive role in AER development. However, when mice exhibiting loss of *Fgf8* in the limb in combination with the removal of other AER-expressed FGFs were examined, progressively more severe phenotypes characterised by the loss of distal limb structures, were observed. It can be concluded that all of the AER FGFs are important for limb development, with *Fgf8* being the most critical, followed (in the order of decreasing importance) by *Fgf4*, *Fgf9* and *Fgf17* (Mariani et al., 2008).

5. *FGF17* in human disease

5.1. *Congenital hypogonadotropic hypogonadism (CHH)/Kallmann Syndrome*

Congenital hypogonadotropic hypogonadism (CHH) is a disorder caused by a deficiency and/or resistance of gonadotropin-releasing hormone (GnRH) (Bianco and Kaiser, 2009; Cangiano et al., 2021). Neurons that secrete GnRH originate in the olfactory placode and migrate into the hypothalamus, accompanied by olfactory neurons (Schwanzel-Fukuda and Pfaff, 1989). Because of the similar migratory pathway and shared signalling mechanisms involved in the development of both the GnRH-secreting and olfactory neurons, 50–60% of CHH cases are accompanied by complete or partial loss of smell (Kallmann syndrome (KS)) (Young et al., 2019). GnRH deficiencies result in low plasma levels of luteinizing hormone (LH) and follicle-stimulating hormone (FSH), which results in low testosterone levels (in males) and oestrogen and progesterone (in females) (Crowley et al., 1985). CHH is clinically characterized by partial/absent puberty, poorly defined secondary sexual characteristics and infertility (Cangiano et al., 2021) in addition to non-reproductive related abnormalities i such as hearing loss, renal aplasia, low bone density and dental agenesis (Cangiano et al., 2021). Approximately 40 genes have been associated with CHH/KS; many of which encode receptor-ligand pairs involved in GnRH neuron development and/or migration (see (Valdes-Socin et al., 2014; Boehm et al., 2015; Cangiano et al., 2021; Swee et al., 2021; Liu and Zhi, 2022) FGFR1 and its associated ligands (FGF8, FGF17, IL17RD, SPRY4, DUSP6 and FLRT3) are among the receptor-ligand pairs implicated in CHH/KS (Miraoui et al., 2013).

FGFR1 is involved in GnRH proliferation and migration and it is essential for initiating olfactory bulb development (Hébert et al., 2003; Cangiano et al., 2021). Mutations in *FGFR1* have been found in approximately 10% of CHH individuals, and non-reproductive related abnormalities such as craniofacial, digit and dental abnormalities are more prevalent in these individuals (Dodé et al., 2003; Jarzabek et al., 2012; Costa-Barbosa et al., 2013). It has been functionally demonstrated that in mice, *Fgf8* plays a role in GnRH neuron development (Falardeau et al., 2008; McCabe et al., 2011; Yellapragada et al., 2022). Furthermore, based on the high sequence homology between *Fgf8* and *Fgf17* (63.7% at the amino acid level) (Maruoka et al., 1998), the overlapping expression domains of *Fgf8* and *Fgf17* in the olfactory placode of mice and the ability of FGF17 to activate FGFR1, *Fgf17* may play a similar role in GnRH neuron development and/or migration, however, this is yet to be demonstrated (Partanen, 2007; Miraoui et al., 2013).

Mutations in *FGF17* account for a relatively small proportion of CHH/KS cases; being present in only 1.1% of screened CHH/KS cohorts (Miraoui et al., 2013; Men et al., 2020; Cangiano et al., 2021) (see Table 2).

FGF17 mutations display an autosomal dominant mode of inheritance, however, considering the broad involvement of the FGF signalling pathway in the pathology of CHH/KS, *FGF17* may also have a digenic contribution in which an individual has two mutant alleles in two different genes (Individual 4 and 7 – Table 2) or an oligogenic contribution in which an individual has more than two mutant alleles in two different genes (Individual 1 -Table 2). Individual 1 has mutations in *FGF17, FGFR1, HS6ST1 and FLRT3*; all are members of the FGF signalling pathway and are implicated in CHH (Amato et al., 2019). *HS6ST1* acts to enzymatically modify heparin sulfate, enabling it to act as a co-factor for FGF17, mediating FGF17 binding and activity to FGFR1 (Brauner et al., 2023). FLRT3 has been shown to interact with FGFR1 and act as a positive regulator of FGF signalling by increasing MAPK signalling (Böttcher et al., 2004; Haines et al., 2006; Partanen, 2007; Miraoui et al., 2013; Latko et al., 2019). Interestingly, this patient and her family members affected by CHH carry three to six mutant alleles in *FGF17*, *FLRT3*, *HS6ST1*, and *FGFR1* whereas asymptomatic family members have zero to two mutant alleles (Miraoui et al., 2013). This suggests that mutations may synergize to produce a more severe phenotype.

FGF17 mutations may also show incomplete penetrance. For example, Individual 6 (Table 2) was diagnosed with CHH, however, the individual's father and one sibling carry the p.K191R mutation in *FGF17* but were unaffected.

Mutations in *FGF17* may also show variable expressivity, where some patients displayed normal puberty (Table 2 - Individual 5,6 and 8) but puberty was absent in others (Table 2 – Individual 2 and 3).

It is interesting to note that while the reproductive structures of *Fgf17*$^{+/-}$ and *Fgf17*$^{-/-}$ mice were not analyzed, both mutants were fertile and showed pubertal development. This may be due to compensation by other FGF members such as *Fgf8*. It would be interesting to see how GnRH neuron development and/or migration is affected by *Fgf17* knockout in *Fgf8*-null mice.

5.2. *Dandy-Walker malformation*

Dandy-Walker malformation (DWM) is a rare congenital cerebellar defect, occurring between 1 in 10 000 o 30 000 births (Santoro et al., 2019). It is characterised by underdevelopment or dysplasia of the

Table 2
FGF17 mutations in patients with Congenital Hypogonadotropic Hypogonadism or Kallmann Syndrome.

Individual, sex	Nucleotide change	Amino acid change	Diagnosis	Phenotype	Mutations in other CHH-or-KS-related genes?	How mutations were detected	Reference
1,F	c.323T > C (heterozygous)	p.Ile108Thr (missense)	KS	• Puberty absent •Low bone mass	Yes – *FLRT3*, *HS6ST1* and *FGFR1*	Direct sequencing of PCR products. Genes involved in the *FGF8* subfamily group were analyzed	Miraoui et al. (2013)
2,M	c.530G > A (heterozygous)	p.Arg177His (missense)	CHH	•Puberty absent •Low bone mass	No		Miraoui et al. (2013)
3,M	c.560A > G (heterozygous)	p.Asn187Ser (missense)	KS	•Puberty absent	No		Miraoui et al. (2013)
4,M		p.48_52del (in-frame deletion)	KS	•Aplasia of olfactory bulb •Pidgeon breast •Hearing loss •Dental agenesis •Mental sweating* •Low bone mass	Yes – *OTUD4*	Whole Exome sequencing	Men et al. (2020)
5,M		p.Pro120Leu	KS	•Anomalous trichromatism •Aplasia of olfactory bulb	No		Men et al. (2020)
6,M		p.Lys191Arg	CHH	•	No		Men et al. (2020)
7,M	c.208G > A (heterozygous)	p.Gly70Arg	KS	•Atrophy of olfactory bulb	Yes –*IL17RD*	Next-generation sequencing with a customized panel of 31 genes designed for CHH/KS	Cannarella et al. (2023)
8,M	c.196G > A (heterozygous)	p.Val66Met	CHH		No	Custom SureSelectXT DNA panel (Agilent Technologies Inc) containing 36 CHH-associated genes	Amato et al. (2019)

Abbreviations: F = female. M = male. KS = Kallmann syndrome. CHH = Congenital Hypogonadotropic Hypogonadism. Low bone mass includes osteopenia, osteoporosis, or fractures. *Mental sweating: sweating every 30 min–1 hour on the head, chest, and abdomen regardless of cold or heat(Men et al., 2020).

cerebellum vermis, expansion of the fourth ventricle and posterior fossa cistern (Monteagudo, 2020). DWM is often associated with various central nervous system (CNS) and non-CNS abnormalities, including those affecting the cardiovascular, digestive, and renal systems, as well as limb and cervicofacial development (Sun et al., 2023).

The genetic basis of DWM remains poorly understood, though several chromosome abnormalities (Imataka et al., 2007) and rare pathogenic gene variants have been identified, such as *FOXC1* (Haldipur et al., 2017), *ZIC1* and *ZIC4* (Blank et al., 2011; Tohyama et al., 2011; Ferraris et al., 2013), *ABL-1* (Garzon et al., 2024), *NID1* (Darbro et al., 2013; Dietvorst et al., 2023) *LAMC1* (Darbro et al., 2013), and *CAPN15* (Beaman et al., 2023). *FGF17* is located on 8p21.3, an area which has been implicated with DWM through chromosome abnormalities such as deletions and inverted duplications (Fan and Siu, 2001; Feenstra et al., 2006; Zanni et al., 2011). However, only one of these reported cases have investigated *FGF17* as a factor involved 8p-related vermis hypoplasia/DWM (Zanni et al., 2011).

Notably, a *de novo* deletion on human chromosome 8p21.2–21.3 (measuring 2.3 Mb), involving *FGF17*, was reported in one patient presenting with DWM (presenting with vermis hypoplasia). Located 1 Mb from the proximal deletion breakpoint, *FGF17* expression was markedly reduced, suggesting the potential influence of long-range elements within the deleted area (Zanni et al., 2011).

A possible mechanism for *FGF17* linked vermis hypoplasia presented in the reported case is described in a mouse model for *Fgf17* and *Fgf8* mutants. Investigation into the roles of *Fgf8* and *Fgf17* in the development of the mouse embryo mid hind brain (MHB) demonstrated a cooperative but partially redundant functions. Both *Fgf8* and *Fgf17* are detected by E8.5, with *Fgf8* being more prominent E8.5 and peaking at E10.5. *Fgf17* increases at this point, while *Fgf8* expression diminishes is undetectable at E14.5. At E14.5, *Fgf17* expression continues to be expressed strongly, with a narrowed expression domain along the MHB junction. In embryos lacking *Fgf17* ($Fgf17^{-/-}$) and in double mutants lacking *Fgf17* and possessing a heterozygous null *Fgf8* ($Fgf17^{-/-}/Fgf8^{\Delta 2,3n/+}$), there was a decrease in overall size and significant loss of the midline vermis tissue, particularly the vermis lobe III, with the double mutant experiencing more severe tissue loss. However, in heterozygous null mutants for both *Fgf17* and *Fgf8* ($Fgf17^{-/+}/Fgf8^{\Delta 2,3n/+}$), the midbrain and cerebellum were normal compared to the wildtype, indicating that *Fgf17* and *Fgf8* function through an autosomal recessive mechanism. Both $Fgf17^{-/-}$ and $Fgf17^{-/-}/Fgf8^{\Delta 2,3n/+}$ exhibited reduced proliferation of the cerebellar precursor cells; corresponding to the degree of tissue loss among the different mutants, indicating that *Fgf8* and *Fgf17* maintain precursor cell proliferation in a dose-dependent manner from E11.5. The loss of vermis lobe III is attributed to the reduced availability of precursor cells (Liu and Ornitz, 2000). Despite the differing mechanisms of *Fgf17* disruption in the mouse model and case study, consistent reduction in *FGF17* expression supports this particular instance of DWM.

How 8p-related inverted duplications contribute to vermis hypoplasia as reported previously (Fan and Siu, 2001; Feenstra et al., 2006) remains unclear. There is variability in the proximal and distal breakpoints for these inverted duplications; proximal breakpoints ranging from 8p11.2 to 8p21.3 and distal breakpoints ranging from 8p21.2 to 8p23.3 (Fan and Siu, 2001; Feenstra et al., 2006). This is apparent in the cases reported by Feenstra et al. (2006), where 6 out of 9 reported cases presented with vermis hypoplasia. Of particular note are patients 5 and 6 who presented with near identical inverted duplication breakpoints (8p11.2 to 8p23.1), however, only patient 6 presented with vermis hypoplasia (Feenstra et al., 2006). It should additionally be noted that 8p-related direct duplications are not associated with any DWM pathology (Engelen et al., 1995, 2000).

FGF17 has been implicated in both DWM and KS/CHH (Ueno et al., 2004; Aluclu et al., 2007). However, despite its involvement in both disorders, there is little to no overlap in primary disorder phenotype; KS/CHH is characterised by hypogonadotropic hypogonadism and anosmia and DWM characterised by cerebellar malformation. Among the two reported cases, one had a normal karyotype with chromosome G banding, and although *KAL1* was investigated, the results were inconclusive (Ueno et al., 2004). The second case, diagnosed with DWM via CT scans, with no reported karyotype or potential gene candidates (Aluclu et al., 2007).

5.3. Chronic Kidney Disease

Chronic Kidney Disease (CKD), characterized by the gradual loss of kidney function is caused by toxins or other health conditions (common ones include: diabetes, hypertension and inherited kidney diseases) that impair kidney function (Kalantar-Zadeh et al., 2021). While hemodialysis is a common treatment for CKD, it is unable to remove all of the uremic toxins. These non-dialyzable uremic toxins contribute to the progression of CKD by causing inflammation, cellular dysfunction and promoting fibrosis in the kidney (van Ham et al., 2022).

In silico modelling of pathological pathways activated in renal tubular cells exposed to post-dialysis uremic plasma vs renal tubular cells exposed to healthy plasma showed that *FGF17* was implicated in pathways associated with inflammation, fibrosis, apoptosis, metabolic dysfunction, and oxidative stress in the renal tubular cells modelling non-dialyzable uremic toxin exposure (Asadi et al., 2024). Although promising, further research exploring the role *FGF17* in CKD is required.

5.4. Pituitary Stalk Interruption Syndrome

Pituitary Stalk Interruption Syndrome (PSIS) is a rare (0.5 cases per 100 000 births) congenital disorder of the pituitary gland, in which there are abnormalities to one/more of the three lobes of the pituitary gland. This results in deficiencies in pituitary hormones that manifest as specific phenotypes. For example, growth hormone deficiency leading to growth retardation and dwarfism (Voutetakis et al., 2016; Wang et al., 2017; Vergier et al., 2019; Voutetakis, 2021).

Whole exome sequencing of patients with PSIS revealed a missense variant (c.C634T:p.P212S) in *FGF17* (Brauner et al., 2023). However, predictive software (Polyphen (Adzhubei et al., 2010) and SIFT (Ng and Henikoff, 2001)) could not determine whether the missense variant was pathogenic or not (Brauner et al., 2023). The patient also had mutations in *GLI2* and *PTCH1* (Brauner et al., 2023). *GLI2* mutations have been associated with PSIS and a growing body of evidence associates *PTCH1* mutations with PSIS (Zwaveling-Soonawala et al., 2018; Brauner et al., 2020; Fang et al., 2020). Given these PSIS-associated-mutations, it is difficult to implicate *FGF17* in PSIS.

While no abnormalities of the pituitary were reported in *Fgf17*$^{+/-}$ and *Fgf17*$^{-/-}$ mice mutants, *Fgf17* transcripts are expressed in the pituitary gland of E12.5 and E14.5 mice embryos, suggesting a possible role in pituitary development (Brinkmeier et al., 20AD; Davis et al., 2013). Additional research is required to implicate *FGF17* in PSIS.

5.5. Cancer

In human cancer, atypical regulation of FGF/FGFR signalling results in abnormal activation of ligand-dependent and ligand-independent FGFR signalling. A wide variety of cancers contain FGF/FGFR aberrations, most commonly presenting as gene amplification and single nucleotide variants with less frequent gene rearrangements of both *FGFR* and FGF family members (Helsten et al., 2016; Krook et al., 2021). FGF/FGFR signalling contributes to all stages of cancer development, such cancer survival and proliferation, angiogenesis, invasion, metastasis and treatment response (Xie et al., 2020).

Expression of *FGF17* has been implicated in several cancers. *FGF17 in prostate cancer*. In the adult prostate, FGF/FGFR signalling acting in autocrine and/or paracrine fashions is critical for maintenance and homeostasis via bidirectional cross-talk between the stroma and epithelial compartments. Alterations in this signalling can initiate/promote carcinogenesis (Giacomini et al., 2021).

FGF17 is expressed at low levels in prostate epithelial cells. As an autocrine factor, it promotes epithelial proliferation, while at higher concentrations, it acts as a paracrine factor to stimulate stromal cell proliferation *in vitro* (Polnaszek et al., 2004). *FGF17* expression was found to be elevated in prostate cancer clinical specimens compared to benign prostate hyperplasia, and there was a further increase in expression levels in high-grade tumours. Patients with tumours with high *FGF17* expression had lower survival rates and higher risk of developing bone metastasis (Heer et al., 2004; Valta et al., 2008). *In vitro* assays showed 1 ng/μl FGF17 to be a highly effective mitogen, showing a significant increase in cell proliferation in several prostate cancer cell lines (LNCaP, DU145, and PC3M) (Heer et al., 2004). *FGF8* is expressed in prostate cancer, with the FGF8b isoform being the predominant splice form (Giacomini et al., 2021), where it has been shown to induce *FGF17* expression and potentially increase *FGF17* expression in the tumour microenvironment (Heer et al., 2004).

FGF17 in hematopoietic cancers. Hematopoietic cancers encompass a range of malignancies affecting the blood, bone marrow and lymphatic system. Increased expression of the *FGF8/17/18* subfamily has been observed in B- and T-lymphoid and myeloid tumour cell lines, as well as in patient samples of acute myeloid leukemia (AML) and acute lymphoblastic leukemia (ALL). *FGF17* was further showed to increase cell proliferation of lymphoma cell lines expressing high affinity *FGF17* receptors (FGFR-2IIIc or 3IIIc) in a dose dependent manner (Nezu et al., 2005). In AML patients, *FGF17* expression was found to be significantly correlated to poor overall survival. Moreover, *FGF17* expression found to be associated with cancer-related pathways such as PI3K-Akt, MAPK, Ras, Rap1 and mTOR which play roles in inhibiting apoptosis, cell cycle progression and stimulating cell proliferation (Ling and Du, 2022).

FGF17 in hepatocellular carcinoma (HCC). HCC is the most prevalent form of primary liver cancer and the fourth leading cause of cancer related deaths worldwide, developing though a stepwise process from chronic hepatitis, liver fibrosis, liver cirrhosis, and, finally, HCC (Alawyia and Constantinou, 2023). In 59% of HCC cases studies, there was observed up-regulation of the *FGF8/17/18* subfamily and their primary receptors (FGFR2,3, and 4). Under conditions mimicking rapid expanding HCC; serum depletion and hypoxia, *in vitro* cell lines increased expression of all *FGF8* subfamily members, which rescued cells from apoptosis via the ERK and Akt/mTOR pathway. The mechanism of induction of *FGF8* and *FGF17* under these conditions, however, remains unclear. All members of the FGF8 subfamily further induced cell proliferation of the tumour stroma cells (myofibroblasts), and via tumour-stroma crosstalk and VEGF (vascular endothelial growth factor) pathways induced tube formation of endothelial cells; acting as a paracrine mechanism for neoangiogenesis (Gauglhofer et al., 2011).

FGF in cervical cancer and perineural invasion (PNI). PNI is the presence of cancer cells that cover the nerve and/or invade any of the three layers of the nerve sheath; the epineurium, perineurium, and endoneurium (Chen et al., 2024). In PNI positive samples from cervical cancer, differential expression analysis identified *ADCYAP1* (encoding PACAP) to be significantly upregulated (Chen et al., 2023). PACAP mediated PNI in cervical cancer involve activation of peripheral nervous system Schwann cells (SC). Usually, PACAP plays a role in Schwann cell (SC) mediated response to nerve damage in the peripheral nervous system, particularly though the activation of SCs (Maugeri et al., 2020) during which they enter a dedifferentiated repair state capable of migration (Wei et al., 2024). *In vitro*, cervical cancer cell lines (HeLa and ME-180) induced a repair-like state of co-cultured SCs via PACAP paracrine signalling. Activated SCs in return induce EMT of HeLa and ME-180 cells. Mechanistically, it was shown that PACAP induced increased expression of *FGF17*, *Cathepsin S* (CTSS) and *MMP-12* in SCs (Chen et al., 2023). FGF/FGFR signalling promotes invasive cervical cancer (Mateus and Wiedlocha, 2022). The exact mechanism by which FGF17 contributes to cell migration is unclear. CTSS and MMP-12 is suggested to promote a microenvironment which facilitates cancer cell dissemination along nerves through EMC degradation as well as degradation of protein components of the perineurium.

FGF17 in clear cell Renal Cell Carcinoma (ccRCC). ccRCC typically originates from the tubular epithelium of the kidney and accounts for approximately 70% of diagnosed renal cell carcinomas (Jonasch et al., 2021). *FGF17*, along with *PRKCG*, *SSTR1*, and *SCTR* were identified to be associated with progression, metastasis and immune response in

ccRCC. qRT-PCR showed a significant *FGF17* increase in two ccRCC cell lines (786-O and caki-1), with the protein being mainly distributed extracellularly. The underlying mechanism of FGF17 mediated cancer progression and metastasis is unclear (Sun et al., 2022), but is likely to function as a paracrine or autocrine factor based on the extracellular localisation of the FGF17 protein.

FGF17 in Glioblastoma. RNA-seq conducted on human glioblastoma (GBMs) and non-cancerous adjacent tissue, taken from 12 patients diagnosed with GBM, showed that *FGF17* was expressed approximately 2-fold lower in GBM compared to non-cancerous adjacent tissue (Zhao et al., 2024).

The 'Survival Analysis' tool' from GEPIA (Tang et al., 2017), was used to evaluate whether the survival of patients with GBM or gliomas was influenced by the expression of *FGF17*. Interestingly, the expression levels of *FGF17* showed no correlation to the survival of patients with GBM ($P = 0.82$), however, high *FGF17* expression showed longer survival ($P < 0.001$) in patients with gliomas (Zhao et al., 2024). (Note: high and low expression was determined based on the median expression). Future research could investigate whether FGF17 protein expression is also aberrant in gliomas and how *FGF17* expression influences the proliferation and metastatic behaviour of gliomas.

6. Summary

The review explores the role of *FGF17*, a member of the *FGF8/17/18* subfamily. We have discussed *Fgf17's* role in mammalian embryonic development, particularly focusing on its functions at the midbrain-hindbrain boundary and in forebrain patterning, limb and facial development. Despite its broad expression, knockout studies in mice reveal relatively mild phenotypes, which are attributed to functional redundancy with the two other member of its subfamily, *Fgf8* and *Fgf18*. These knockout mice exhibited reductions in the size of brain structures of the inferior colliculus and vermis cerebellum, as well as abnormalities in social behaviours likely attributed to altered forebrain patterning. *FGF17* is also implicated in human diseases. Mutations in *FGF17* have been linked to congenital hypogonadotropic hypogonadism (CHH)/ Kallmann Syndrome, as well as Dandy-Walker malformation.

The overlapping roles of the *FGF8/17/18* subfamily could be investigated by examining single knockouts of *Fgf8*, *Fgf17*, and *Fgf18* alongside a triple knockout could help clarify the specific role of *Fgf17* during development, as *Fgf17* mutant mice do not completely reflect the phenotype observed in humans with *FGF17* mutations.

FGF17 expression is elevated in several cancers, including prostate cancer, hematopoietic cancers, and hepatocellular carcinoma, cervical cancer, renal cell carcinoma and gliomas. However, the underlying mechanism by which FGF17 contributes to different cancer types is unknown and requires further research. The therapeutic potential of FGF17 has also been considered, in neuroprotection during ischemic stroke and its ability to improve cognitive function in aging mice. The therapeutic applications of FGF17, combined with its involvement in various pathologies, underscore the need for continued research to fully understand its functions and potential as a therapeutic target.

CRediT authorship contribution statement

Zane Oberholzer: Writing – original draft, Writing – review & editing. **Chiron Loubser:** Writing – original draft, Writing – review & editing. **Natalya V. Nikitina:** Writing – original draft, Writing – review & editing.

References

Abramyan, J., 2015. Lineage-specific loss of FGF17 within the avian orders Galliformes and Passeriformes. Gene 563 (2), 180–189. https://doi.org/10.1016/J.GENE.2015.03.027.

Adzhubei, IvanA., et al., 2010. A method and server for predicting damaging missense mutations. Nat. Methods 7 (4), 248–249. https://doi.org/10.1016/0002-9343(63)90102-5.

Alawyia, B., Constantinou, C., 2023. Hepatocellular carcinoma: a narrative review on current knowledge and future prospects. Curr. Treat. Options Oncol. 24 (7), 711–724. https://doi.org/10.1007/s11864-023-01098-9.

Alkayed, N.J., Cipolla, M.J., 2023. The ever-evolving concept of the neurovascular unit. Stroke 54 (8), 2178–2180. https://doi.org/10.1161/STROKEAHA.123.042705.

Aluclu, M.U., Bahceci, S., Bahceci, M., 2007. A rare embryological malformation of brain - Dandy-Walker syndrome - and its association with Kallmann's syndrome. Neuroendocrinol. Lett. 28 (3), 255–258.

Amato, L.G.L., Montenegro, L.R., Lerario, A.M., Jorge, A.A.L., Guerra Junior, G., et al., 2019. New genetic findings in a large cohort of congenital hypogonadotropic hypogonadism. Eur. J. Endocrinol. 181 (2), 103–119. https://doi.org/10.1530/EJE-18-0764.

Asadi, R., Shadpour, P., Nakhaei, A., 2024. Non-dialyzable uremic toxins and renal tubular cell damage in CKD patients: a systems biology approach. Eur. J. Med. Res. 29 (1), 412. https://doi.org/10.1186/s40001-024-01951-z.

Bachler, M., Neubüser, A., 2001. Expression of members of the Fgf family and their receptors during midfacial development. Mech. Dev. 100 (2), 313–316. https://doi.org/10.1016/S0925-4773(00)00518-9.

Bally-Cuif, L., Wassef, M., 1995. Determination events in the nervous system of the vertebrate embryo. Curr. Opin. Genet. Dev. 5 (4), 450–458. https://doi.org/10.1016/0959-437X(95)90048-L.

Beaman, M.M., et al., 2023. Novel association of Dandy–Walker malformation with CAPN15 variants expands the phenotype of oculogastrointestinal neurodevelopmental syndrome. Am. J. Med. Genet. 191 (11), 2757–2767. https://doi.org/10.1002/ajmg.a.63363.

Bianco, S.D.C., Kaiser, U.B., 2009. The genetic and molecular basis of idiopathic hypogonadotropic hypogonadism. Nat. Rev. Endocrinol. 5 (10), 569–576. https://doi.org/10.1038/nrendo.2009.177.

Blank, M.C., et al., 2011. Multiple developmental programs are altered by loss of Zic1 and Zic4 to cause Dandy-Walker malformation cerebellar pathogenesis. Development 138 (6), 1207–1216. https://doi.org/10.1242/dev.054114.

Boehm, U., et al., 2015. Expert consensus document: European Consensus Statement on congenital hypogonadotropic hypogonadism-pathogenesis, diagnosis and treatment. Nature Reviews Endocrinology. Nature Publishing Group, pp. 547–564. https://doi.org/10.1038/nrendo.2015.112.

Böttcher, R.T., et al., 2004. The transmembrane protein XFLRT3 forms a complex with FGF receptors and promotes FGF signalling. Nat. Cell Biol. 6 (1), 38–44. https://doi.org/10.1038/ncb1082.

Boylan, M., et al., 2020. The Fgf8 subfamily (Fgf8, Fgf17 and Fgf18) is required for closure of the embryonic ventral body wall. Development (Camb.) 147 (21). https://doi.org/10.1242/dev.189506.

Brauner, R., et al., 2020. Pituitary stalk interruption syndrome is characterized by genetic heterogeneity. PLoS One 15 (12), e0242358. https://doi.org/10.1371/journal.pone.0242358.

Brauner, R., et al., 2023. Exome sequencing in 16 patients with pituitary stalk interruption syndrome: a monocentric study. PLoS One 18 (12), e0292664. https://doi.org/10.1371/journal.pone.0292664.

Brinkmeier, M. et al. (20AD) 'Discovery of transcriptional regulators and signaling pathways in the developing pituitary gland by bioinformatic and genomic approaches', Genomics, 93(5), pp. 449–460. Available at: https://doi.org/10.1016/j.ygeno.2008.11.010.Discovery.

Campbell, B.C.V., et al., 2019. Ischaemic stroke. Nat. Rev. Dis. Prim. 5 (1). https://doi.org/10.1038/s41572-019-0118-8.

Cangiano, B., et al., 2021. Genetics of congenital hypogonadotropic hypogonadism: peculiarities and phenotype of an oligogenic disease. In: Human Genetics. Springer Berlin Heidelberg. https://doi.org/10.1007/s00439-020-02147-1.

Cannarella, R., et al., 2023. Genetic analysis of patients with congenital hypogonadotropic hypogonadism: a case series. Int. J. Mol. Sci. 24 (8), 1–17. https://doi.org/10.3390/ijms24087428.

Cao, Y., et al., 2004. fgf17b, a novel member of Fgf family, helps patterning zebrafish embryos. Dev. Biol. 271 (1), 130–143. https://doi.org/10.1016/j.ydbio.2004.03.032.

Charbonnier, G., et al., 2021. Intracranial bleeding after reperfusion therapy in acute ischemic stroke. Front. Neurol. 11. https://doi.org/10.3389/fneur.2020.629920.

Chen, G., et al., 2023. Dedifferentiated Schwann cells promote perineural invasion mediated by the PACAP paracrine signalling in cervical cancer. J. Cell Mol. Med. 27 (23), 3692–3705. https://doi.org/10.1111/jcmm.17897.

Chen, G., et al., 2024. Perineural invasion in cervical cancer: a hidden trail for metastasis. Diagnostics 14 (14), 1517. https://doi.org/10.3390/diagnostics14141517.

Chi, C.L., et al., 2003. The isthmic organizer signal FGF8 is required for cell survival in the prospective midbrain and cerebellum. Development 130 (12), 2633–2644. https://doi.org/10.1242/dev.00487.

Cholfin, J.A., Rubenstein, J.L.R., 2007. Patterning of frontal cortex subdivisions by Fgf17. Proc. Natl. Acad. Sci. U. S. A. 104 (18), 7652–7657. https://doi.org/10.1073/pnas.0702225104.

Cholfin, J.A., Rubenstein, J.L.R., 2008. Frontal cortex subdivision patterning is coordinately regulated by Fgf8, Fgf17, and Emx2. J. Comp. Neurol. 509 (2), 144–155. https://doi.org/10.1002/cne.21709.

Costa-Barbosa, F.A., et al., 2013. Prioritizing genetic testing in patients with kallmann syndrome using clinical phenotypes. J. Clin. Endocrinol. Metab. 98 (5), 943–953. https://doi.org/10.1210/jc.2012-4116.

Crowley, W.F., et al., 1985. The physiology of gonadotropin-releasing hormone (GnRH) secretion in men and women. Recent Progress in Hormone Research. ACADEMIC PRESS, INC. https://doi.org/10.1016/b978-0-12-571141-8.50015-9
Darbro, B.W., et al., 2013. Mutations in extracellular matrix genes NID1 and LAMC1 cause autosomal dominant dandy-walker malformation and occipital cephaloceles. Hum. Mutat. 34 (8), 1075–1079. https://doi.org/10.1002/humu.22351.
Davis, S., et al., 2013. Pituitary gland development and disease: from stem cell to hormone production. Curr. Top. Dev. Biol. 106 (1), 1–47. https://doi.org/10.1016/j.coph.2007.10.002.Taste.
Dietvorst, S., et al., 2023. NID1-related autosomal dominant Dandy-Walker malformation with occipital cephalocele in three generations. Eur. J. Med. Genet. 66 (4), 104713. https://doi.org/10.1016/j.ejmg.2023.104713.
Dodé, C., et al., 2003. Loss-of-function mutations in FGFR1 cause autosomal dominant Kallmann syndrome. Nat. Genet. 33 (4), 463–465. https://doi.org/10.1038/ng1122.
Dordoe, C., et al., 2021. Roles of fibroblast growth factors and their therapeutic potential in treatment of ischemic stroke. In: Frontiers in Pharmacology. Frontiers Media S.A. https://doi.org/10.3389/fphar.2021.671131.
Eblaghie, M.C., et al., 2004. Interactions between FGF and Wnt signals and Tbx3 gene expression in mammary gland initiation in mouse embryos. J. Anat. 205 (1), 1–13. https://doi.org/10.1111/j.0021-8782.2004.00309.x.
Engelen, J.J.M., et al., 1995. Familial partial trisomy 8p without dysmorphic features and only mild mental retardation. J. Med. Genet. 32 (10), 792–795. https://doi.org/10.1136/jmg.32.10.792.
Engelen, J.J.M., et al., 2000. Duplication of chromosome region 8p23.1-p23.3: a benign variant? Am. J. Med. Genet. 91 (1), 18–21. https://doi.org/10.1002/(SICI)1096-8628(20000306)91:1<18::AID-AJMG3>3.0.CO;2-3.
Falardeau, J., et al., 2008. Decreased FGF8 signaling causes deficiency of gonadotropin-releasing hormone in humans and mice. J. Clin. Invest. 118 (8), 2822–2831. https://doi.org/10.1172/JCI34538.
Fan, Y.-S., Siu, V.M., 2001. Molecular cytogenetic characterization of a derivative chromosome 8 with an inverted duplication of 8p21.3?p23.3 and a rearranged duplication of 8q24.13?qter. Am. J. Med. Genet. 102 (3), 266–271. https://doi.org/10.1002/ajmg.1460.
Fang, X., et al., 2020. Identification of novel candidate pathogenic genes in pituitary stalk interruption syndrome by whole-exome sequencing. J. Cell Mol. Med. 24 (20), 11703–11717.
Feenstra, I., et al., 2006. Neuroimaging in nine patients with inversion duplication of the short arm of chromosome 8. Neuropediatrics 37 (2), 83–87. https://doi.org/10.1055/s-2006-924108.
Ferraris, A., et al., 2013. Dandy-Walker malformation and Wisconsin syndrome: novel cases add further insight into the genotype-phenotype correlations of 3q23q25 deletions. Orphanet J. Rare Dis. 8 (1), 75. https://doi.org/10.1186/1750-1172-8-75.
Garzon, J.P., et al., 2024. Dandy–Walker malformation in an individual with ABL1 variant. Am. J. Med. Genet. https://doi.org/10.1002/ajmg.a.63718 [Preprint].
Gauglhofer, C., et al., 2011. Up-regulation of the fibroblast growth factor 8 subfamily in human hepatocellular carcinoma for cell survival and neoangiogenesis. Hepatology 53 (3), 854–864. https://doi.org/10.1002/hep.24099.
Giacomini, A., et al., 2021. The FGF/FGFR system in the physiopathology of the prostate gland. Physiol. Rev. 101 (2), 569–610. https://doi.org/10.1152/physrev.00005.2020.
Goldman, D.C., Martin, G.R., Tam, P.P.L., 2000. Fate and function of the ventral ectodermal ridge during mouse tail development. Development 127 (10), 2113–2123. https://doi.org/10.1242/dev.127.10.2113.
Goutam, R.S., et al., 2023. Exploring the structural and functional diversity among fgf signals: a comparative study of human, mouse, and Xenopus fgf ligands in embryonic development and cancer pathogenesis. Int. J. Mol. Sci. 24 (8), 7556. https://doi.org/10.3390/IJMS24087556, 2023, Vol. 24, Page 7556.
Gruters, K.G., Groh, J.M., 2012. Sounds and beyond: multisensory and other non-auditory signals in the inferior colliculus. Front. Neural Circ. 6 (NOV), 1–39. https://doi.org/10.3389/FNCIR.2012.00096/BIBTEX.
Haines, B.P., et al., 2006. Regulated expression of FLRT genes implies a functional role in the regulation of FGF signalling during mouse development. Dev. Biol. 297 (1), 14–25. https://doi.org/10.1016/j.ydbio.2006.04.004.
Haldipur, P., et al., 2017. Phenotypic outcomes in Mouse and Human Foxc1 dependent Dandy-Walker cerebellar malformation suggest shared mechanisms. Elife 6. https://doi.org/10.7554/eLife.20898.
van Ham, W.B., Cornelissen, C.M., van Veen, T.A.B., 2022. Uremic toxins in chronic kidney disease highlight a fundamental gap in understanding their detrimental effects on cardiac electrophysiology and arrhythmogenesis. Acta Physiol. 236 (3), 1–14. https://doi.org/10.1111/apha.13888.
Hasenpusch-Theil, K., Watson, J.A., Theil, T., 2017. Direct interactions between Gli3, Wnt8b, and fgfs underlie patterning of the dorsal telencephalon. Cerebr. Cortex 27 (2), 1137–1148. https://doi.org/10.1093/cercor/bhv291.
Haupt, M., et al., 2022. Quest for quality in translational stroke research—a new dawn for neuroprotection? Int. J. Mol. Sci. 23 (10), 5381. https://doi.org/10.3390/ijms23105381.
Haupt, M., et al., 2023. Neuroprotective strategies for ischemic stroke—future perspectives. Int. J. Mol. Sci. 24 (5), 4334. https://doi.org/10.3390/ijms24054334.
Hébert, J.M., et al., 2003. FGF signaling through FGFR1 is required for olfactory bulb morphogenesis. Development 130 (6), 1101–1111. https://doi.org/10.1242/dev.00334.
Heer, R., et al., 2004. Fibroblast growth factor 17 is over-expressed in human prostate cancer. J. Pathol. 204 (5), 578–586. https://doi.org/10.1002/path.1668.
Helsten, T., et al., 2016. The FGFR landscape in cancer: analysis of 4,853 tumors by next-generation sequencing. Clin. Cancer Res. 22 (1), 259–267. https://doi.org/10.1158/1078-0432.CCR-14-3212.
Hoch, R.V., Clarke, J.A., Rubenstein, J.L.R., 2015. Fgf signaling controls the telencephalic distribution of Fgf-expressing progenitors generated in the rostral patterning center. Neural Dev. 10 (1). https://doi.org/10.1186/s13064-015-0037-7.
Hoshikawa, M., et al., 1998. Structure and expression of a novel fibroblast growth factor, FGF-I7, preferentially expressed in the embryonic brain. Biochem. Biophys. Res. Commun. 244 (1), 187–191. https://doi.org/10.1006/bbrc.1998.8239.
Huang, W.T., et al., 2024. FGF17 protects cerebral ischemia reperfusion-induced blood-brain barrier disruption via FGF receptor 3-mediated PI3K/AKT signaling pathway. Eur. J. Pharmacol. 971. https://doi.org/10.1016/j.ejphar.2024.176521.
Imataka, G., Yamanouchi, H., Arisaka, O., 2007. Dandy-Walker syndrome and chromosomal abnormalities. Congenital. Anom. 47 (4), 113–118. https://doi.org/10.1111/j.1741-4520.2007.00158.x.
Iram, T., et al., 2022. Young CSF restores oligodendrogenesis and memory in aged mice via Fgf17. Nature 605, 509–515. https://doi.org/10.1038/s41586-022-04722-0.
Itoh, N., Ornitz, D.M., 2008. Functional evolutionary history of the mouse Fgf gene family. Dev. Dynam. 237 (1), 18–27. https://doi.org/10.1002/dvdy.21388.
Jarzabek, K., et al., 2012. Evidence that FGFR1 loss-of-function mutations may cause variable skeletal malformations in patients with Kallmann syndrome. Adv. Med. Sci. 57 (2), 314–321. https://doi.org/10.2478/v10039-012-0036-4.
Jin, S., Choe, C.P., 2024. A potential role of fgf4, fgf24, and fgf17 in pharyngeal pouch formation in zebrafish. Develop. Reproduct. 28 (2), 55–65. https://doi.org/10.12717/DR.2024.28.2.55.
Jonasch, E., Walker, C.L., Rathmell, W.K., 2021. Clear cell renal cell carcinoma ontogeny and mechanisms of lethality. Nat. Rev. Nephrol. 17 (4), 245–261. https://doi.org/10.1038/s41581-020-00359-2.
Jovelin, R., et al., 2007. Duplication and divergence of fgf8 functions in teleost development and evolution. J. Exp. Zool. B Mol. Dev. Evol. 308 (6), 730–743. https://doi.org/10.1002/jez.b.21193.
Jovelin, R., et al., 2010. Evolution of developmental regulation in the vertebrate FgfD subfamily. J. Exp. Zool. B Mol. Dev. Evol. 314 (1), 33–56. https://doi.org/10.1002/jez.b.21307.
Kadry, H., Noorani, B., Cucullo, L., 2020. A blood–brain barrier overview on structure, function, impairment, and biomarkers of integrity. Fluids Barr. CNS. BioMed Central Ltd. https://doi.org/10.1186/s12987-020-00230-3.
Kalantar-Zadeh, K., et al., 2021. Chronic kidney disease. Lancet 398 (10302), 786–802. https://doi.org/10.1016/S0140-6736(21)00519-5.
Kettunen, P., et al., 2011. Developmentally regulated expression of intracellular Fgf11-13, hormone-like Fgf15 and canonical Fgf16, -17 and -20 mRNAs in the developing mouse molar tooth. Acta Odontol. Scand. 69 (6), 360–366. https://doi.org/10.3109/00016357.2011.568968.
Krook, M.A., et al., 2021. Fibroblast growth factor receptors in cancer: genetic alterations, diagnostics, therapeutic targets and mechanisms of resistance. Br. J. Cancer 124 (5), 880–892. https://doi.org/10.1038/s41416-020-01157-0.
Latko, M., et al., 2019. Cross-talk between fibroblast growth factor receptors and other cell surface proteins. Cells. Faculty of Biotechnology, Department of Protein Engineering, University of Wroclaw, Joliot-Curie 14a, 50-383 Wroclaw, Poland. marta.latko2@uwr.edu.pl. https://doi.org/10.3390/cells8050455.
Lea, R., et al., 2009. Temporal and spatial expression of FGF ligands and receptors during Xenopus development. Dev. Dynam. 238 (6), 1467–1479. https://doi.org/10.1002/dvdy.21913.
Lee, S.M.K., et al., 1997. Evidence that FGF8 signalling from the midbrain-hindbrain junction regulates growth and polarity in the developing midbrain. Development 124 (5), 959–969. https://doi.org/10.1242/DEV.124.5.959.
Lewandoski, M., Sun, X., Martin, G.R., 2000. Fgf8 signalling from the AER is essential for normal limb development. Nat. Genet. 26 (4), 460–463. https://doi.org/10.1038/82609.
Li, Y., et al., 2016. Heparin binding preference and structures in the fibroblast growth factor family parallel their evolutionary diversification. Open Biology 6 (3), 150275. https://doi.org/10.1098/rsob.150275.
Ling, Y., Du, Q., 2022. FGF10/FGF17 as prognostic and drug response markers in acute myeloid leukemia. Current Res. Translat. Med. 70 (1), 103316. https://doi.org/10.1016/j.retram.2021.103316.
Liu, A., et al., 2003. FGF17b and FGF18 have different midbrain regulatory properties from FGF8b or activated FGF receptors. Development 130 (25), 6175–6185. https://doi.org/10.1242/DEV.00845.
Liu, A., Joyner, A.L., 2001. Early anterior/posterior patterning of the midbrain and cerebellum. Annu. Rev. Neurosci. 24, 869–896.
Liu, J.X.Z., Ornitz, D.M., 2000. Temporal and spatial gradients of Fgf8 and Fgf17 regulate proliferation and differentiation of midline cerebellar structures. Development 127 (9), 1833–1843. https://doi.org/10.1242/dev.127.9.1833.
Liu, Y., Zhi, X., 2022. Advances in genetic diagnosis of kallmann syndrome and genetic interruption. Reprod. Sci. 29 (6), 1697–1709. https://doi.org/10.1007/s43032-021-00638-8/Published.
Loboda, A., et al., 2016. Role of Nrf2/HO-1 system in development, oxidative stress response and diseases: an evolutionarily conserved mechanism. Cell. Mol. Life Sci. 73 (17), 3221–3247. https://doi.org/10.1007/s00018-016-2223-0.
Malheiros, J.M., et al., 2015. Manganese-enhanced MRI: biological applications in neuroscience. Front. Neurol. 6 (161), 1–10. https://doi.org/10.3389/fneur.2015.00161.
Mariani, F.V., Ahn, C.P., Martin, G.R., 2008. Genetic evidence that FGFs play an instructive role in limb proximal-distal patterning. Nature 453 (7193), 401–405. https://doi.org/10.1038/nature06876.
Maruoka, Y., et al., 1998. Comparison of the expression of three highly related genes, Fgf8, Fgf17 and Fgf18, in the mouse embryo. Mech. Dev. 74 (1–2), 175–177. https://doi.org/10.1016/S0925-4773(98)00061-6.

Masoli, S., Solinas, S., D'Angelo, E., 2015. Action potential processing in a detailed Purkinje cell model reveals a critical role for axonal compartmentalization. Front. Cell. Neurosci. 9, 1–22. https://doi.org/10.3389/fncel.2015.00047.
Mateus, D., Wiedlocha, A., 2022. FGF–FGFR signaling promotes the development of invasive cervical cancer. FEBS J. 289 (12), 3419–3421. https://doi.org/10.1111/febs.16384.
Maugeri, G., et al., 2020. Effects of PACAP on Schwann cells: focus on nerve injury. Int. J. Mol. Sci. 21 (21), 8233. https://doi.org/10.3390/ijms21218233.
McCabe, M.J., et al., 2011. Novel FGF8 mutations associated with recessive holoprosencephaly, craniofacial defects, and hypothalamo-pituitary dysfunction. J. Clin. Endocrinol. Metab. 96 (10), 1709–1718. https://doi.org/10.1210/jc.2011-0454.
McConnell, H.L., Mishra, A., 2022. Cells of the blood–brain barrier: an overview of the neurovascular unit in health and disease. In: Methods in Molecular Biology. Humana Press Inc., pp. 3–24. https://doi.org/10.1007/978-1-0716-2289-6_1
Men, M., et al., 2020. Genotypic and phenotypic spectra of FGFR1, FGF8, and FGF17 mutations in a Chinese cohort with idiopathic hypogonadotropic hypogonadism. Fertil. Steril. 113 (1), 158–166. https://doi.org/10.1016/j.fertnstert.2019.08.069.
Meulemans, D., Bronner-Fraser, M., 2007. Insights from amphioxus into the evolution of vertebrate cartilage. PLoS One 2 (8), e787. https://doi.org/10.1371/journal.pone.0000787.
Miraoui, H., et al., 2013. Mutations in FGF17, IL17RD, DUSP6, SPRY4, and FLRT3 are identified in individuals with congenital hypogonadotropic hypogonadism. Am. J. Hum. Genet. 92 (5), 725–743. https://doi.org/10.1016/j.ajhg.2013.04.008.
Mitchell, J.P., Macrae, C.N., Banaji, M.R., 2006. Dissociable medial prefrontal contributions to judgments of similar and dissimilar others. Neuron 50 (4), 655–663. https://doi.org/10.1016/j.neuron.2006.03.040.
Mohammadi, M., Olsen, S.K., Ibrahimi, O.A., 2005. Structural basis for fibroblast growth factor receptor activation. Cytokine Growth Factor Rev. 16 (2), 107–137. https://doi.org/10.1016/j.cytogfr.2005.01.008.
Monteagudo, A., 2020. Dandy-walker malformation. Am. J. Obstet. Gynecol. 223 (6), B38–B41. https://doi.org/10.1016/j.ajog.2020.08.184.
Morgan, J.I., Curran, T., 1989. Stimulus-transcription coupling in neurons: role of cellular immediate-early genes. Trends Neurosci. 12 (11), 459–462. https://doi.org/10.1016/0166-2236(89)90096-9.
Nezu, M., et al., 2005. Expression of the fetal-oncogenic fibroblast growth factor-8/17/18 subfamily in human hematopoietic tumors. Biochem. Biophys. Res. Commun. 335 (3), 843–849. https://doi.org/10.1016/j.bbrc.2005.07.153.
Ng, P.C., Henikoff, S., 2001. Predicting deleterious amino acid substitutions. Genome Res. 11 (5), 863–874. https://doi.org/10.1101/gr.176601.
Okada, T., et al., 2019. FGF-2 attenuates neuronal apoptosis via FGFR3/PI3k/akt signaling pathway after subarachnoid hemorrhage. Mol. Neurobiol. 56 (12), 8203–8219. https://doi.org/10.1007/s12035-019-01668-9.
Olsen, S.K., et al., 2006. Structural basis by which alternative splicing modulates the organizer activity of FGF8 in the brain. Gene Dev. 20 (2), 185–198. https://doi.org/10.1101/gad.1365406.
Ornitz, D.M., Itoh, N., 2015. The fibroblast growth factor signaling pathway. WIREs Dev. Biol. 4 (3), 215–266. https://doi.org/10.1002/wdev.176.
Park, I.S., Lee, N.J., Rhyu, I.J., 2018. Roles of the declive, folium, and tuber cerebellar vermian lobules in sportspeople. J. Clin. Neurol. 14 (1), 1–7. https://doi.org/10.3988/jcn.2018.14.1.1.
Partanen, J., 2007. FGF signalling pathways in development of the midbrain and anterior hindbrain. J. Neurochem. 101 (5), 1185–1193. https://doi.org/10.1111/j.1471-4159.2007.04463.x.
Polnaszek, N., et al., 2004. FGF17 is an autocrine prostatic epithelial growth factor and is upregulated in benign prostatic hyperplasia. Prostate 60 (1), 18–24. https://doi.org/10.1002/pros.20026.
Porntaveetus, T., et al., 2011. Expression of fibroblast growth factors (Fgfs) in murine tooth development. J. Anat. 218 (5), 534–543. https://doi.org/10.1111/j.1469-7580.2011.01352.x.
Qin, C., et al., 2022. Signaling pathways involved in ischemic stroke: molecular mechanisms and therapeutic interventions. Signal Transduct. Targeted Ther. 7 (1), 215. https://doi.org/10.1038/s41392-022-01064-1.
Raman, R., Sasisekharan, V., Sasisekharan, R., 2005. Structural Insights into biological roles of protein-glycosaminoglycan interactions. Chem. Biol. 12 (3), 267–277. https://doi.org/10.1016/j.chembiol.2004.11.020.
Reifers, F., et al., 2000. Overlapping and distinct functions provided by fgf17, a new zebrafish member of the Fgf8/17/18 subgroup of Fgfs. Mech. Dev. 99 (1–2), 39–49. https://doi.org/10.1016/S0925-4773(00)00475-5.
Saddam, Md, et al., 2024. Emerging biomarkers and potential therapeutics of the BCL-2 protein family: the apoptotic and anti-apoptotic context. Egyptian J. Med. Human Genetics 25 (1), 12. https://doi.org/10.1186/s43042-024-00485-7.
Salaudeen, M.A., et al., 2024. Understanding the pathophysiology of ischemic stroke: the basis of current therapies and opportunity for new ones. In: Biomolecules. Multidisciplinary Digital Publishing Institute. https://doi.org/10.3390/biom14030305 (MDPI).
Santoro, M., et al., 2019. Epidemiology of dandy-walker malformation in europe: a EUROCAT population-based registry study. Neuroepidemiology 53 (3–4), 169–179. https://doi.org/10.1159/000501238.
Satou, Y., Imai, K.S., Satoh, N., 2002. Fgf genes in the basal chordate Ciona intestinalis. Dev. Gene. Evol. 212 (9), 432–438. https://doi.org/10.1007/s00427-002-0266-8.
Scearce-Levie, K., et al., 2008. Abnormal social behaviors in mice lacking Fgf17. Gene Brain Behav. 7 (3), 344–354. https://doi.org/10.1111/j.1601-183X.2007.00357.x.
Schwanzel-Fukuda, M., Pfaff, D.W., 1989. Origin of luteinizing hormone-releasing hormone neurons. Nature 338 (6211), 161–164. https://doi.org/10.1038/338161a0.
Soldozy, S., et al., 2023. Reperfusion injury in acute ischemic stroke: tackling the irony of revascularization. Clin. Neurol. Neurosurg. 225, 107574. https://doi.org/10.1016/j.clineuro.2022.107574.
Sun, S., et al., 2022. Metastatic immune-related genes for affecting prognosis and immune response in renal clear cell carcinoma. Front. Mol. Biosci. 8. https://doi.org/10.3389/fmolb.2021.794326.
Sun, X., et al., 2000. Conditional inactivation of Fgf4 reveals complexity of signalling during limb bud development. Nat. Genet. 25 (1), 83–86. https://doi.org/10.1038/75644.
Sun, Y., et al., 2023. Clinical features and genetic analysis of Dandy-Walker syndrome. BMC Pregnancy Childbirth 23 (1), 40. https://doi.org/10.1186/s12884-023-05367-1.
Swee, D.S., Quinton, R., Maggi, R., 2021. Recent advances in understanding and managing Kallmann syndrome. Fac Rev 10 (37).
Tacer, K.F., et al., 2010. Research resource: comprehensive expression atlas of the fibroblast growth factor system in adult mouse. Mol. Endocrinol. 24 (10), 2050–2064. https://doi.org/10.1210/ME.2010-0142.
Tang, Z., et al., 2017. GEPIA: a web server for cancer and normal gene expression profiling and interactive analyses. Nucleic Acids Res. 45 (W1), W98–W102. https://doi.org/10.1093/nar/gkx247.
Tohyama, J., et al., 2011. Dandy–Walker malformation associated with heterozygous ZIC1 and ZIC4 deletion: report of a new patient. Am. J. Med. Genet. 155 (1), 130–133. https://doi.org/10.1002/ajmg.a.33652.
Ueno, H., et al., 2004. A case of kallmann syndrome associated with dandy-walker malformation. Exp. Clin. Endocrinol. Diabetes 112 (1), 62–67. https://doi.org/10.1055/s-2004-815728.
Valdes-Socin, H., et al., 2014. Reproduction, smell, and neurodevelopmental disorders: genetic defects in different hypogonadotropic hypogonadal syndromes. Front. Endocrinol. 5 (JUL), 93010. https://doi.org/10.3389/FENDO.2014.00109/BIBTEX.
Valta, M.P., et al., 2008. FGF-8 is involved in bone metastasis of prostate cancer. Int. J. Cancer 123 (1), 22–31. https://doi.org/10.1002/ijc.23422.
Vergier, J., et al., 2019. Pituitary stalk interruption syndrome: etiology and clinical manifestations. Eur. J. Endocrinol. 181 (5), R199–R209. https://doi.org/10.1530/EJE-19-0168.
Visel, A., et al., 2007. VISTA Enhancer Browser - a database of tissue-specific human enhancers. Nucleic Acids Res. 35 (Suppl. 1), 88–92. https://doi.org/10.1093/nar/gkl822.
Voutetakis, A., 2021. Chapter 2 - pituitary stalk interruption syndrome. In: Swaab, D.F., et al. (Eds.), Handbook of Clinical Neurology. Elsevier (Handbook of Clinical Neurology), pp. 9–27. 10.1016/B978-0-12-820683-6.00002-6.
Voutetakis, A., Sertedaki, A., Dacou-Voutetakis, C., 2016. Pituitary stalk interruption syndrome: cause, clinical manifestations, diagnosis, and management. Curr. Opin. Pediatr. 28 (4), 545–550. https://doi.org/10.1097/MOP.0000000000000378.
Wang, C.Z., et al., 2017. Pituitary stalk interruption syndrome: from clinical findings to pathogenesis. J. Neuroendocrinol. 29 (1). https://doi.org/10.1111/jne.12451.
Wang, L., et al., 2024. Comprehensive review of tenecteplase for thrombolysis in acute ischemic stroke. J. Am. Heart Assoc. 13 (9). https://doi.org/10.1161/JAHA.123.031692.
Wei, C., et al., 2024. Advances of Schwann cells in peripheral nerve regeneration: from mechanism to cell therapy. Biomed. Pharmacother. 175, 116645. https://doi.org/10.1016/j.biopha.2024.116645.
Xie, Y., et al., 2020. FGF/FGFR signaling in health and disease. Signal Transduct. Targeted Ther. 5 (1), 181. https://doi.org/10.1038/s41392-020-00222-7.
Xiong, Y., Wakhloo, A.K., Fisher, M., 2022. Advances in acute ischemic stroke therapy. Circ. Res. 130 (8), 1230–1251. https://doi.org/10.1161/CIRCRESAHA.121.319948.
Xu, J., et al., 1999. Genomic structure, mapping, activity and expression of fibroblast growth factor 17. Mech. Dev. 83 (1–2), 165–178. https://doi.org/10.1016/S0925-4773(99)00034-9.
Xu, J., Liu, Z., Ornitz, D.M., 2000. Temporal and spatial gradients of Fgf8 and Fgf17 regulate proliferation and differentiation of midline cerebellar structures. Development 127 (9), 1833–1843. https://doi.org/10.1242/dev.127.9.1833.
Xue, S., et al., 2023. Stroke-induced damage on the blood–brain barrier. In: Frontiers in Neurology. Frontiers Media SA. https://doi.org/10.3389/fneur.2023.1248970.
Yaguchi, Y., et al., 2009. Fibroblast growth factor (FGF) gene expression in the developing cerebellum suggests multiple roles for FGF signaling during cerebellar morphogenesis and development. Dev. Dynam. 238 (8), 2058–2072. https://doi.org/10.1002/DVDY.22013.
Yellapragada, V., et al., 2022. FGF8–FGFR1 signaling regulates human GnRH neuron differentiation in a time- and dose-dependent manner. Dis. Models Mech. 15 (8). https://doi.org/10.1242/DMM.049436.
Young, J., et al., 2019. Clinical management of congenital hypogonadotropic hypogonadism. Endocr. Rev. 40 (2), 669–710. https://doi.org/10.1210/er.2018-00116.
Yu, X., et al., 2005. In vivo auditory brain mapping in mice with Mn-enhanced MRI. Nat. Neurosci. 8 (7), 961–968. https://doi.org/10.1038/nn1477.
Yu, X., et al., 2011. Morphological and functional midbrain phenotypes in Fibroblast Growth Factor 17 mutant mice detected by Mn-enhanced MRI. Neuroimage 56 (3), 1251–1258. https://doi.org/10.1016/j.neuroimage.2011.02.068.
Zanni, G., et al., 2011. FGF17, a gene involved in cerebellar development, is downregulated in a patient with Dandy-Walker malformation carrying a de novo 8p deletion. Neurogenetics 12 (3), 241–245. https://doi.org/10.1007/s10048-011-0283-8.

Zhang, X., et al., 2006. Receptor specificity of the fibroblast growth factor family: the complete mammalian FGF family. J. Biol. Chem. 281 (23), 15694–15700. https://doi.org/10.1074/jbc.M601252200.

Zhao, K., Xu, J., Zhao, B., 2024. Panoramic RNA expression of fibroblast growth factors in human glioblastoma tissues and the impact on the survival of patients. Oncol. Lett. 28 (317), 1–9. https://doi.org/10.3892/ol.2024.14450.

Zwaveling-Soonawala, N., et al., 2018. Clues for polygenic inheritance of pituitary stalk interruption syndrome from exome sequencing in 20 patients. J. Clin. Endocrinol. Metab. 103 (2), 415–428. https://doi.org/10.1210/jc.2017-01660.